CHANGES IN THE RPB3 INTERACTOME CAUSED BY THE DELETION OF RPB9 IN *SACCHAROMYCES CEREVISIAE*

Eric A Talbert

Submitted to the faculty of the University Graduate School
in partial fulfillment of the requirements
for the degree
Master of Science
in Biochemistry and Molecular Biology
Indiana University

August 2016

Accepted by the Graduate Faculty, Indiana University, in partial

fulfillment of the requirements for the degree of Master of Science

Master's Thesis Committee

_____

Amber L. Mosley, PhD. Chair

_____

Mark G. Goebl, PhD.

_____

Andy Hudmon, PhD

ACKNOWLEDGEMENTS

I wish to extend my heartfelt thanks to the following people for their aid completing this project. It would not have been possible without their help.

- To Dr. Amber Mosley- For taking me in and helping me make the best of a bad situation, and for being patient and kind when that was the most important thing in the world.
- To Dr. Mark Goebl- For being a constant source of guidance and mentorship throughout my time with the Biochemistry Department.
- To Dr. Andy Hudmon- For being a teacher and mentor, and also a friend.
- To my colleagues in the Mosley Lab, Whitney Smith-Kinnaman, Dr. Melanie Fox, Dr. Jerry Hunter, Sarah Peck, and Jose Victorino- For your help and instruction, as well as the use of your data.
- To my parents, Larry and Margaret Talbert- For your unwavering love and support throughout my life.
- To my sister, Dr. Erin Talbert- For your advice and mentorship, and for lending an ear when I needed one.

Eric A Talbert

CHANGES IN THE RPB3 INTERACTOME CAUSED BY THE DELETION OF RPB9 IN *SACCHAROMYCES CEREVISIAE*

RNA Polymerase II (Pol II) is the primary actor in the transcription of mRNA from genes. Pol II is a complex composed of twelve protein subunits. This study focused on the changes in the interactome of Rbp3 in *S. cerevisiae* when the Pol II subunit Rpb9 is removed. Rpb3 is one of the core subunits of Pol II, and any significant changes to the Rpb3 incteractome due to the loss of Rpb9 can be used to infer new information about Rpb9's role in the Pol II complex.

Rpb3 was pulled down using FLAG purification from both wild type and *rpb9Δ S. cerevisiae* cultures. Rpb3 and the proteins complexed with it were then analyzed using multi-dimensional protein identification technology (MudPIT), a form of liquid chromatography-mass spectrometry (LC-MS). This data was searched using the SEQUEST database search algorithm, and the results were further analyzed for likelihood of interaction using Significance Analysis of INTeractome (SAINT), as well as for post-translational phosphorylation. Deletion of *rpb9* did not present any changes in Pol II phosphorylation however it did cause several changes in the interaction network. The *rpb9Δ* strain showed new interactions with Rtr1, Sen1, Vtc4, Pyc1, Tgl4, Sec61, Tfb2, Hfd1, Erv25, Rib4, Sla1, Ubp15, Bbc1, and Hxk1. The most prominent of these hits are Rtr1, an Rpb1 C-terminal domain phosphatase linked to transcription termination, and Sen1, an RNA/DNA nuclease that terminates transcription. In addition, this mutant showed no interaction with Mtd1, an interaction that is present in the wild type. In all cases, these hits should be considered fuel for future research, rather than conclusive evidence of novel interactions.

Amber L Mosley, PhD Chair

TABLE OF CONTENTS

LIST OF TABLES

LIST OF FIGURES

INTRODUCTION

Genes and Gene Expression

Transcription is the process of transforming genetic information stored within DNA into functional RNA molecules. These molecules perform a variety of roles within the cell, from structural and catalytic functions in ribosomes to blueprints for the synthesis of proteins. In all cases, however, transcription starts with a DNA template.

DNA is a polymer of nucleotides that serves as the primary information storage medium for living cells. DNA chains form a distinctive double-helix shape, with two phospho-sugar chains linked together by nitrogenous bases, forming a set of rungs on the twisted ladder of the DNA molecule. The sequence of these base pairs makes up a code that contains the actual genetic information stored within DNA (Watson, 1953).

A section of DNA that codes for a specific functional product is called a gene. Genes are the primary target of transcription. Genes can be divided into several sections based on function. Most notable of these is the transcribed region, which is the stretch of DNA that is copied during transcription. The first point of the transcribed region is called the transcription start site (TSS). Promoters are regions upstream of the TSS that interact directly or indirectly with the transcription complex, the group of proteins that, when bound together, perform transcription (Bayev, 1980). Most genes contain a core promoter region just upstream of the TSS. This is the binding site of the preinitiation complex, a grouping of proteins that work together to initiate transcription. Along with this core promoter, many promoter regions also contain enhancer elements that are bound by transcriptional activators, which are other proteins that encourage transcription of the gene (Bran, 1985).

Much of an organism's genome functions to regulate gene expression, or how and when genes are transcribed. In addition to transcriptional activators discussed above, some of this control comes from how DNA molecules are organized into structures called chromosomes. While prokaryote genomes are generally contained within one or a few chromosomes, eukaryotic organisms have multiple large, linear chromosomes. Because of their length, each chromosome is packed into multiple nucleosomes, genetic structures formed by winding a section of DNA around several proteins called histones. How a chromosome is packed into nucleosomes affects what DNA is available for transcription (Cedar, 1976).

Like DNA, RNA is a polymer of nucleotides. However, RNA is made up of ribonucleotide monomers, rather than the deoxyribonucleotide monomers of DNA. The presence of a second hydroxyl group in these monomers causes ribonucleotide monomers to form and break bonds more easily than deoxyribonucleotides. RNA polymers are therefore significantly less stable than DNA (Brenner, 1961).

Three forms of RNA, messenger RNA (mRNA), transfer RNA (tRNA), and ribosomal RNA (rRNA), are directly responsible for converting the linear genetic information coded in DNA into proteins. Messenger RNA is transcribed from DNA and used as a working copy of the gene to produce the encoded protein (Brenner, 1961). Transfer RNA are RNAs with a looped structure that shuttle amino acids to growing peptides. Each tRNA binds to a specific amino acid. Correct amino acids are added to grown peptides using a three nucleotide sequence that complements the next three nucleotides in the mRNA template, called a codon. Translation, the process of translating the genetic code from an RNA transcript into a protein, occurs within specialized structures called ribosomes which form on mRNAs needing to be translated. tRNAs enter the ribosome and match to the bases of mRNA, delivering the needed amino acid during protein synthesis (Crick, 1968). Ribosomal RNA makes up the largest part of ribosomes, performing

both catalytic and structural functions in the cell's protein synthesis machinery (Wimberley, 2000).

Transcription

Transcription is the production of an RNA copy of a section of DNA. As discussed above, this is vital because although DNA is an extremely stable long-term storage molecule, unless that information can be extracted into a useful form, the information stored within genes cannot be expressed. Transcription allows the cell to make use of the instructions stored within its genome as needed.

Transcription is performed by a group of protein complexes called RNA polymerases. Ribonucleotides are matched by their bases to a DNA template and fused into a polymer chain, forming an RNA transcript (Sentenac, 1985). In prokaryotes, all transcription is handled by a single type of polymerase. However, in eukaryotes, different RNA polymerases transcribe different classes of RNA. In *S. cerevisiae*, the three polymerases are RNA polymerase I, II, and III. The majority of rRNA is transcribed by RNA polymerase I (Pol I). RNA polymerase II (Pol II), transcribes mRNA. RNA polymerase III (Pol III) synthesizes both tRNA and the 5S rRNA.

Pol II is the primary catalyst of mRNA synthesis, and thus the key link between DNA and protein synthesis. While Pol II contains all the machinery necessary to synthesize mRNA, the complex cannot perform transcription unaided (Myer, 1998). Numerous other proteins are involved in mRNA transcription. Transcription is an extremely complex process, and is not fully understood. However, the process can be broken down into three phases: initiation, elongation, and termination. A brief overview of mRNA transcription is presented in Figure 1.

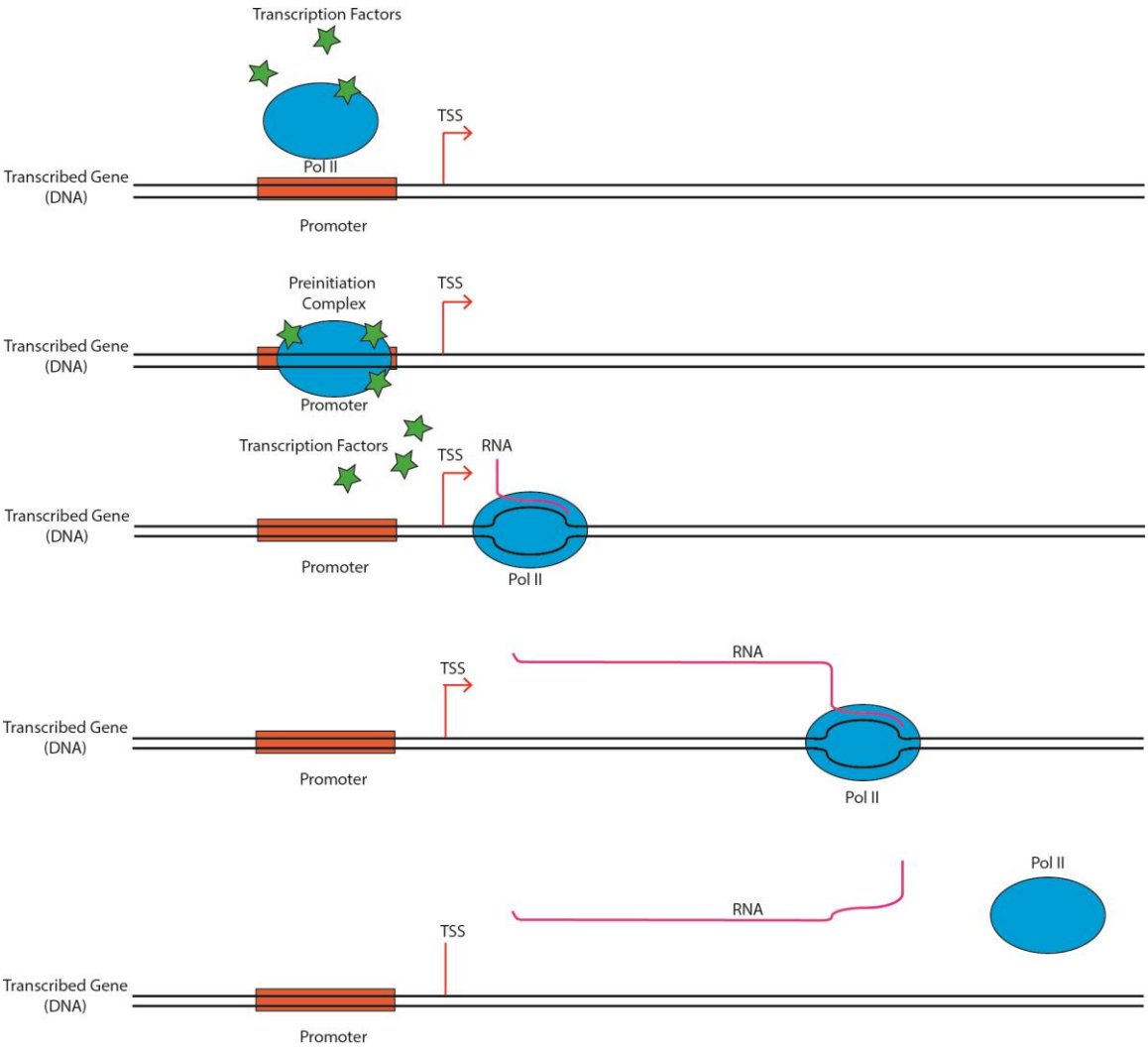

Figure 1: Transcription of Messenger RNA: Transcription factors (green) bind Pol II (blue) and assist in finding and binding the core promoter (orange) of the transcribed gene (black). These transcription factors dissociate from the complex as Pol II adds the first few nucleotides to the nascent RNA molecule (magenta). Transcription transitions into elongation as Pol II continues to move along the gene adding nucleotides to the transcript. Eventually a termination sequence is received, and Pol II releases both the transcript and the transcribed gene.

Transcription initiation is the process of forming the preinitiation complex and preparing the gene for transcription. In most eukaryotic genes, this process begins when TATA binding protein (TBP), as part of the general transcription factor (GTF) TFIID, binds to the core promoter, a region adjacent to the TSS. GTFs are a class of protein complexes that help position RNA polymerases at the promoter and prepare the DNA for transcription. GTFs associated with Pol II use the nomenclature TFII.

After binding the core promoter, TFIID deforms DNA in a way that encourages strand separation, or melting. TFIIB then binds to TFIID and the promoter region, stabilizing the complex. Meanwhile, TFIIF binds and stabilizes Pol II, preparing the complex for recruitment to the promoter site by TFIIB. TFIIB then forms a bridge between the DNA-TFIID complex and Pol II. TFIIE binds to the nascent pre-initiation complex (PIC), stabilizing the PIC further and beginning the process of DNA melting. The 5'-3' DNA helicase TFIIH then binds to PIC. The helicase activity of TFIIH fully melts the TSS, allowing Pol II to begin transcription. Pol II matches free ribonucleotides the bases of the template DNA, fusing the monomers binding the first phosphate of the 5' end of the initial ribonucleotide to the hydroxyl group on the 3' end of the next monomer. After approximately 12 bases have been added to the nascent RNA molecule, the GTFs dissociate from the complex, and elongation begins (Woychik, 2002). The process of transcription initiation is detailed below in Figure 2.

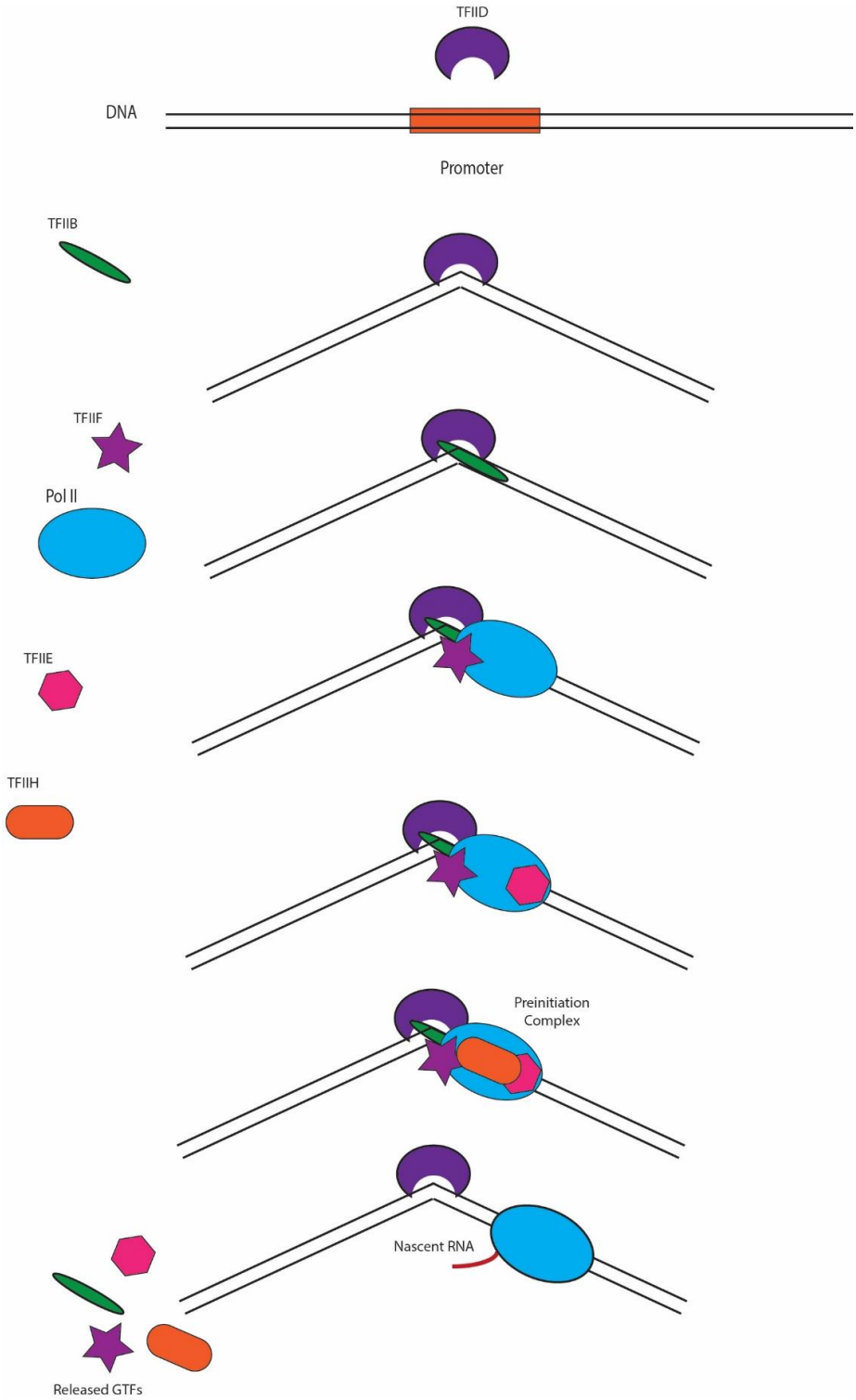

Figure 2: Initiation of Messenger RNA Transcription: TFIID (purple) binds the core promoter (orange), deforming the DNA strand (black). TFIIB (green) binds and stabilizes the TFIID-DNA complex. TFIIF (purple star) binds Pol II (blue), stabilizing the complex. TFIIB binds Pol II, bridging gap the between promoter and Pol II. TFIIE (pink) binds PIC, encourages DNA melting. TFIIH (orange) binds PIC, unwinding DNA to allow Pol II access to the coding strand. Pol II begins transcribing gene. After approximately 12 genes have been added, the GTFs dissociate from the PIC, leaving Pol II to begin elongation.

Elongation is the extension of the short mRNA transcript created during initiation. During this period the majority of bases are added to an mRNA molecule. Like initiation, elongation is regulated by a number of additional factors acting on Pol II. However, unlike initiation, these interactions are much more variable, and there is not a single clear model that can be applied to most elongation events. However, a recurring theme throughout transcription that continues in elongation is the modification of the C-terminal domain (CTD) of Rpb1, the largest subunit of Pol II. Rpb1 ends in a long, unstructured region of 25-52 repeats of the amino acid sequence $Y_1S_2P_3T_4S_5P_6S_7$ (West, 1995). Post-translational modifications (PTMs), and especially phosphorylation of this region are responsible for modulating the activity of the protein and therefore regulating both transcription and cotranscriptional events such as mRNA processing (Corden, 1990).

Termination is the final step of transcription. Transcription is completed when the transcription complex reaches a termination site, a point in the gene that encourages Pol II to dissociate from the DNA template. However, termination can also occur prematurely for a number of reasons, including misincorporation of bases to the transcript, or because Pol II has reached an obstruction and cannot continue along the gene.

As with elongation, phosphorylation of the Rpb1 CTD plays a large role in regulation of termination. Several kinases and phosphatases target the CTD during elongation and termination. Most notable for this study is the phosphatase Rtr1. When elongation begins, the majority of the fifth serine of the CTD heptapeptide repeat (S-5) are phosphorylated by the kinase Kin28. As elongation continues S-5 phosphorylation becomes less common, and is almost nonexistent at the beginning of termination (Komarnitsky, 2000; Figure 3). Rtr1 is a phosphatase that targets S-5 during early RNAPII transcription elongation, removing the phosphate from serine 5 in the CTD repeats (Mosley, 2009).

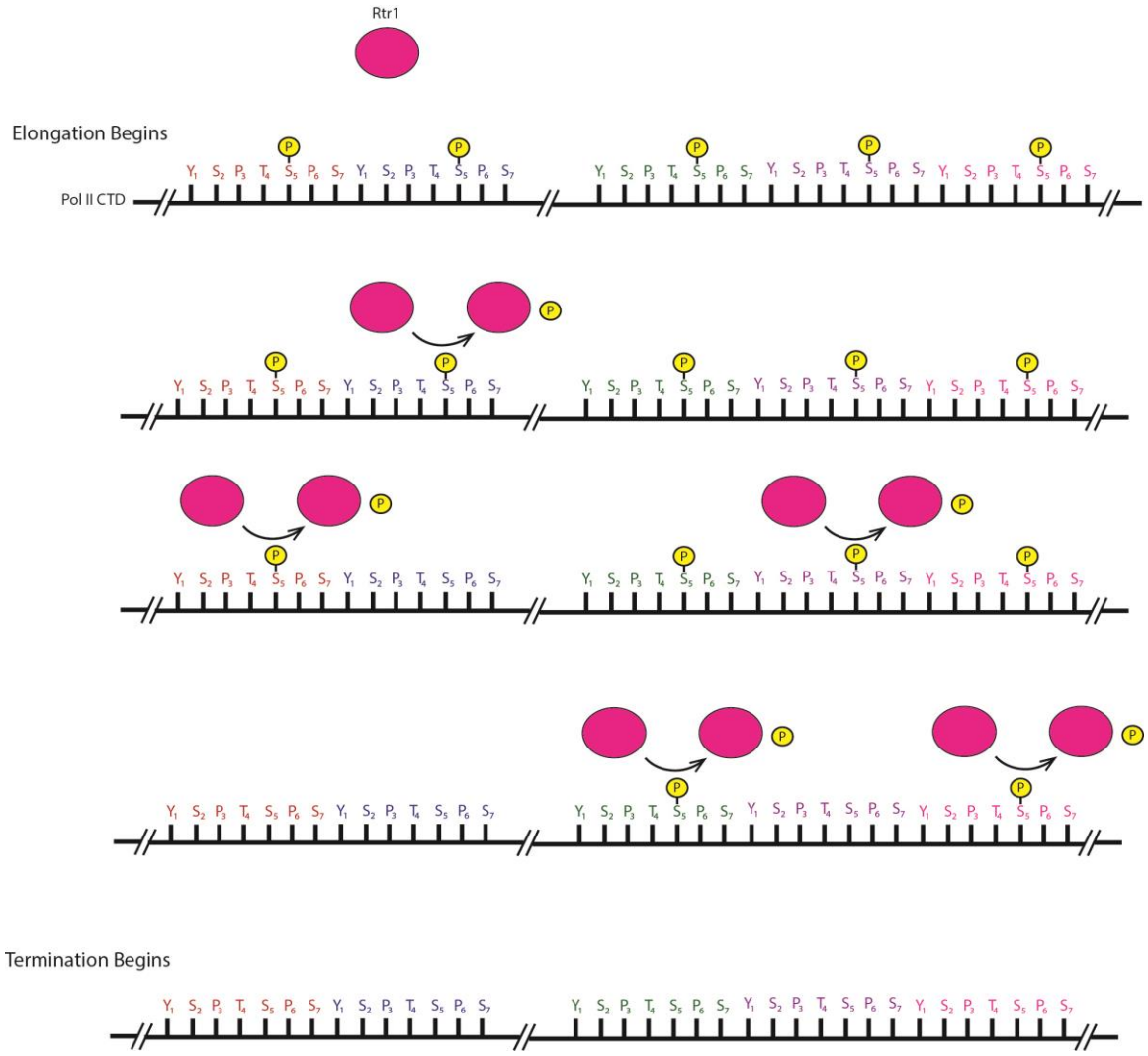

Figure 3: Changes in Phosphorylation State of Serine-5 of the RNA Polymerase II CTD Heptapeptide: At the start of transcription elongation, the Pol II CTD heptapeptide repeat (black) is heavy phosphorylated (yell) at S-5. Rtr1 (magenta) removes these phosphate groups as elongation progresses. Termination becomes more likely as fewer S-5 residues are phosphorylated.

RNA Polymerase II Function

Pol II is the evolutionarily conserved complex of proteins responsible for the transcription of mRNA. In yeast the Pol II complex contains 12 subunits and has a molecular weight of approximately 550 kDa (Cramer, 2002; Figure 4). As mentioned above, Pol II requires a number of additional factors to successfully perform transcription. Often these proteins complex with Pol II, and can be isolated from a cell lysate using an affinity pulldown protocol, allowing for the identification of interacting partners. Our chosen target for this affinity pulldown is Rpb3, a protein at the core of Pol II which has been used for purification of Pol II for multiple previous studies by our group (Mosley, 2009; Mosley, 2011; Mosley 2013).

Rpb3 is a core subunit of yeast Pol II. At 318 amino acids, Rpb3 is the third largest subunit of the complex, and has been shown to be part of a core DNA binding sub-assembly (Kimura, 1997). Rpb3 is vital for the overall stability of the Pol II complex, as it interacts with multiple other Pol II subunits (Kimura, 2000). Additionally, while some subunits are found in all three RNA polymerases, Rpb3 is unique to Pol II (Cramer, 2002). These traits make Rpb3 an excellent target to study the changes in Pol II's protein network when the complex is artificially disrupted, such as when Rpb9 is removed.

Rpb9 is a relatively small subunit of Pol II, at only 122 residues in yeast, and is highly conserved through eukaryotes. It is located at the tip of the "jaws" formed by Rpb1 and Rpb2, placing it near the active site of transcription (Cramer, 2000; Figure 4). While removal of Rpb9 from Pol II complex is nonlethal, this causes a significant reduction in the overall viability of the cells. Deletion of the *rpb9* gene causes both heat and cold sensitivity, and slowed growth even in ideal conditions (Woychik, 1991). Strains lacking *rpb9* also show significant inconsistencies in transcription start site selection (McKune, 1995). In addition, *rpb9Δ* cells show a much lower

tolerance for freeze-thaw stress, showing significantly slower growth after freezing at -25˚C than WT after the same stress, even when normalized against unfrozen controls (Ando, 2007).

In vitro Rpb9, along with TFIIS, was shown to be necessary for Pol II cleavage from sites of transcription arrest, ending a failed transcription event (Awrey, 1997). *In vivo*, *rpb9Δ* cells are sensitive to the drug 6-azauracil, (Hemming, 2000). This phenotype has previously been associated with transcription elongation defects in cells lacking *dst1*, the gene encoding TFIIS. (Exinger, 1992). Overexpression of *dst1* has also been shown to rescue 6-azauracil sensitivity in *rpb9Δ* cells, implying Rpb9 has a role in regulating elongation through an interaction with TFIIS (Hemming, 2000).

In addition to a role in termination, Rpb9 is also active in the maintenance of Pol II transcription fidelity. A study used *can1*, which encodespermease that uptakes both arginine and the toxic arginine analogue cananavine, and a nonsense mutant *can1-100* that significantly reduced cananavine sensitivity, to measure the transcription fidelity effects of Rpb9. Deletion of *rpb9* showed a significant increase in cananavine sensitivity in the *can1-100* mutant, due to increased read-throughs of the premature stope codon (Nesser, 2006). This same study also showed that sequenced cDNA from *rpb9Δ* cells showed an error rate of 2.0×10^{-13} misincorporations per nucleotide, compared to 1.4×10^{-13} for WT cells. Rpb9 has since been shown to be required for two checkpoints events during transcription, one immediately following misincorporation of an NTP and another one nucleotide downstream of the incorrect NTP (Knippa, 2013).

Rpb9 has also been shown to play a role in the transcription coupled repair (TCR) of DNA. TCR in *S. cerevisiae* has been linked to Pol II stalling during transcription, such as might occur when the complex meets a lesion on the coding strand (Hanawalt, 2001). Rpb9 has been found

to mediate one of the two TCR pathways in yeast, a pathway primarily active within the coding region of genes (Li, 2002).

Rpb9 is non-essential in yeast. As such, deleting *rpb9* is a viable genetic perturbation. My central hypothesis for this work is that removing Rpb9 from the Pol II complex will force a number of compensations within the cell, significantly altering the Rpb3 interactome. The changes in this interactome should produce new inferences about Rpb9's role in transcription and the Pol II complex.

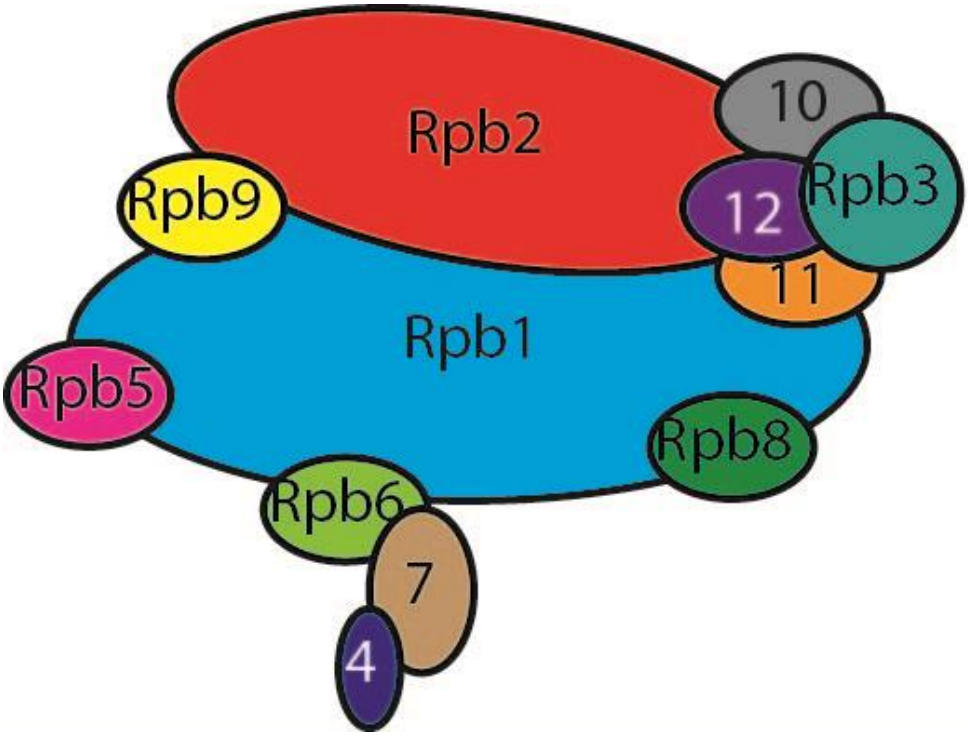

Figure 4: Schematic of RNA Polymerase II Holoenzyme: Note the position of Rpb9 between Rpb1 and Rpb2.

Rpb1	Largest subunit of Pol II. Part of central catalytic core. Activity of complex regulated by phosphorylation of CTD.
Rpb2	Subunit of Pol II. Part of central catalytic core.
Rpb3	Subunit of Pol II. Forms DNA binding structure and contributes to stability of Pol II complex.
Rpb4	Nonessential subunit of Pol II. Forms dimer with Rpb7 associated with temperature response.
Rpb5	Subunit found in all three RNA polymerases. Interacts with DNA during transcription.
Rpb6	Subunit found in all three RNA polymerases. Part of catalytic core.
Rpb7	Subunit of Pol II. Forms dimer with Rpb4 associated with temperature response.
Rpb8	Subunit found in all three RNA polymerases.
Rpb9	Nonessential subunit of Pol II. Associated with transcription fidelity and transcription coupled DNA repair.
Rpb10	Subunit found in all three RNA polymerases.
Rpb11	Subunit of Pol II. Forms part of central catalytic core.
Rpb12	Subunit found in all three RNA polymerases. Associated with DNA damage response.
TFIIB	Pol II transcription factor. Stabilizes TFIID-DNA complex, recruits Pol II to preinitiation complex.
TFIID	Pol II transcription factor. Binds and deforms core promoter DNA to initiate transcription.
TFIIE	Pol II transcription factor. Stabilizes transcription factor-Pol II preinitiation complex.
TFIIF	Pol II transcription factor. Stabilizes Pol II complex, helps to recruit Pol II to TFIIB.
TFIIH	Pol II transcription factor. DNA helicase that opens DNA to allow Pol II access to base pairs.
TBP	Binds core promoter in most transcription events. Part of the TFIID complex in mRNA transcription
Rtr1	Serine phosphatase that targets S-5 of the Rpb1 CTD heptapeptide repeat

Table 1: Selected Actors in mRNA Transcription

MATERIALS AND METHODS

Bioinformatics

The primary principle of bioinformatics is the use of high-throughput techniques to produce large volumes of data coupled with computational tools such as database searches that reduce the time necessary to analyze this data, allowing relatively quick turnaround times. It can be difficult to obtain high-resolution data from some of these methods. They are, however, perfect for narrowing general areas of interest into specific research questions. Bioinformatic tools are a tremendous aid in developing new lines of inquiry. The ability to analyze large volumes of data in a relatively short period of time means trends can be established with relatively little effort. Here we have analyzed interactions in the transcription machinery to discover novel avenues of investigation.

Affinity Purification

Affinity purification is the use of a specific interaction to separate a desired material from a biochemical mixture. While there are several forms of this currently in use, tandem affinity purification (TAP) was used for this study. TAP makes use of a fusion protein made up of the protein of interest and an affinity tag. Chromatography is performed on a cell lysate from a culture expressing the fusion protein, with a resin made up of individual agarose beads, each bound to an antibody against the chosen epitope tag. This allows any proteins complexed with the fusion protein to be pulled down along with the bait from the protein mixture (Westermarck, 2013).

A FLAG tag was chosen for this investigation. FLAG is an eight peptide tag consisting of the sequence DYKDDDDK. FLAG was used because pull downs using this tag will extract both tightly bound proteins found in stable complexes and loosely bound proteins associated with dynamic

interactions. Using the traditional TAP tag, a calmodulin binding peptide, a two-step purification is required, which has been found to pull down only very tightly complexed proteins (Gavin, 2011).

Multidimensional Protein Identification Technology

Multidimensional Protein Identification Technology (MudPIT) pairs liquid chromatography with tandem mass spectrometry to identify the components of a complex protein mixture (Wolters, 2001). MudPIT uses multi-phase high-pressure liquid chromatography (HPLC) columns to separate peptides to make certain they are ionized individually. Typically reverse-phase and strong cation exchange (SCX) materials are used, in either bi- or tri-phasic microcapillary columns (Florens, 2006).

Liquid chromatography, including HPLC, relies on the differences in polarity between the components of a mixture. This is accomplished by using a solid stationary phase packed into a column to initially capture the mixture. A mobile phase of a solvent is then run through the column. In reverse-phase chromatography used here, this mobile phase is initially a polar solvent, in this case water, while the stationary phase is hydrophobic. A second, less polar solvent, such as acetonitrile, is slowly exchanged for the first mobile phase. This gradient means that as the purification progresses, the mobile phase becomes less polar, causing progressively more hydrophobic compounds to elute off the column. In this way the most polar parts of a mixture are eluted first, while the most hydrophobic leave the column at the end of the gradient.

Treating a protein mixture with a protease creates shorter, more easily measured peptides. However, the resultant peptides are simply an amino acid chain with varied side chains, they have very similar hydrophobicities and will elute closely together. Traditionally increasing

separation on the column has been accomplished by increasing the column volume, usually column length. However, with extremely close eluting molecules this can require impractically long columns. Multi-phase columns containing two or more stationary phases allow for separation of molecules with very close hydrophobicity.

Reverse phase stationary phases consist of a highly packed, inert hydrophobic material. In practice, this means silica embedded with simple carbon molecules, usually C8 or C18. These materials allow for a slow enough flow of liquid through the column for molecules to adhere to the column during loading, and the hydrophobicity means the polar-to-non-polar gradient of the mobile phase to elute molecules of different polarity gradually.

SCX resins operate somewhat differently. These resins are embedded with a molecule containing an acidic group. In an aqueous environment, the negative charge of this group attracts molecules with a complementary charge. As the mobile phase becomes less polar, individual anions in the resin lose their charge, until eventually even perfectly complementary cations will lose attraction to the acidic groups and elute (Edelmann, 2011).

Once a specific peptide elutes from the column, the peptide is subjected to tandem mass spectrometry (MS/MS). Mass spectrometry uses the time it takes an ionized molecule to move a specific distance to judge its mass, and by inference its identity. Tandem mass spectrometry uses multiple mass spectrometry runs, interrupted by additional fragmentation of the analyte. This gives the masses of not only the initial molecule, but also a number of fragments that can be used to infer the mass of individual components. This is extremely useful for the identification of proteins, because the sequence of individual peptides can be inferred from this data.

Peptide Spectra Analysis

A discussion of the algorithms used to identify proteins detected in MudPIT spectra is beyond this work, but an understanding of the fundamentals of this approach will be useful in reading this work. The mass of the original short peptide and all fragment ions are used to construct possible sequences for the precursor peptide. A protein database is then searched with an algorithm such as SEQUEST for sequences with a similar mass to the precursor. The matched sequences are further vetted using cross-correlation to compare the mass-to-charge ratio of the precursor to that of the sequences found in the database search (Eng, 1994).

In addition to identifying proteins, the data from MudPIT can be used to find post translational modifications (PTMs) of specific amino acids. Protein searches can be modified to search for the masses of commonly modified amino acids, such as phosphothreonine. In addition, phosphate and some other PTMs are often lost during the fragmentation process, causing a mass shift in the spectra of modified residues. This work utilized PhosphoRS, a piece of software that calculates the probability of phosphorylation at individual sites from MS/MS spectra.

Significance Analysis of INTeractome

Significance Analysis of INTeractome (SAINT) is an open source method for examining protein-protein interactions. SAINT uses Bayesian analysis to score the likelihood of a data set illustrating a valid interaction between two proteins.

$$p(A|B) = p(B|A)p(A)/p(B)$$

Bayesian statistics is based on Baye's Theorem, listed above. Briefly, Baye's Theorem states that the probability that A is true, given that B is true, is equal to the probability that B is true,

given A is known to be true, multiplied by the dividend of the probability of A being true divided by the probability of B being true (Ellenburg, 2014). The details of the application of this theorem as applied in SAINT are beyond this work. A full explanation can be found in Choi, et. al (2006).

Isolation of Protein Fractions from FLAG Tagged *S. cerevisiae*

Two yeast strains isogenic to BY4741 were used in this study, a wild type strain and a knock out for *rpb9* from the Open Biosystems yeast knockout collection. Prior to this study, a sequence 3x-FLAG tag was inserted into the Rpb3 gene of both strains using a tagging cassette from the plasmid pBS1539. Both strains were streaked for isolation on separate yeast extract peptone dextrose (YPD, Table 2) media plates. These plates were grown overnight at room temperature. Single colonies from each strain were used to inoculate 35mL suspension cultures in YPD media, which were grown overnight at 30˚C. 3L of YPD were inoculated from each of these starters. These cultures were likewise grown overnight at 30˚C to final OD600s ranging from 2-4.

Cells from these cultures were harvested by centrifugation at 4,000 x g for 5 minutes at 4°C. These cell pellets were then resuspended in TAP lysis buffer (Table 2). Approximately 250 µL of glass beads were added to this lysis mixture, and the whole was vortexed intermittently at 4˚C for 20 minutes to ensure mechanical lysis. The cell lysate was centrifuged at 12,000 x g for 60 minutes at 4°C to enrich for soluble proteins.

Yeast Extract Peptone Dextrose (YPD) Media (3L)	TAP Lysis Buffer (100 mL)
60g Yeast Extract	40mL 40mM Hepes-NaOH pH 7.5
30g Peptone	100mL 10% Glycerol
270mL milliQ Water	70mL 350mM NaCL
300mL sterile 20% Glucose	1 mL 0.1% Tween-20
	214.25 milliQ water

Table 2: Reagents and Media

Pulldown and Digestion of Protein Fraction

The resulting protein fraction was mixed with 500µL of a FLAG resin and stirred overnight at 4˚C. This suspension was transferred to a Bio-Rad Econoprep column and drained by gravity flow to remove unbound proteins. 60mL of TAP lysis buffer, followed by 25mL of 50mM ammonium bicarbonate (pH=8.0) were then run through the column to further wash the beads.

The beads containing the protein mixture of interest were resuspended in 50mM ammonium bicarbonate. Trypsin Gold was added to a final concentration of 0.0016 µg/µL. The digest was shaken overnight at 37˚C. Mixture was then transferred to a micro-spin column and centrifuged at 10,000 rpm for 2 minutes. 20µL of 90% formic acid was added to the flow through to stop digestion.

MudPIT Analyses

MudPIT analysis was performed on the protein enriched fraction. The HPLC was performed by pressure loading 100 µm silica microcapillary columns with 2 µm reverse phase resin (C18 Aqua), 3 µm strong cation exchange (Luna SCX) resin, and then an additional 8 µm of reverse phase resin at the tip to form three-phase columns. Aliquots of approximately 125 µl of the samples described above were pressure-loaded onto these columns, which were then equilibrated with a 5% acetonitrile, 0.1% formic acid solution.

Dual phase liquid chromatography, tandem mass spectrometry was then performed on the samples. Chromatographic separation was accomplished using a 10 step salt ladder of 50-350mM ammonium acetate preceding an organic gradient of 20-80% acetonitrile with a constant 0.1% formic acid content. Each step on the ladder was eluted into a Thermofisher TLQ Velos for mass spectrometry. The ten most intense ions from this first MS were subjected to fragmentation by collision induced dissociation (CID) and MS/MS. Two technical replicates were performed for each of two separate biological replicates of this procedure, for a total of four replicates for each variable. Thermo Xcalibur software was used to automate the chromatographic separation, elution, and peptide fragmentation.

Analysis of MS/MS Spectra

The RAW spectra files were searched with Thermo's Proteome Discoverer 1.4, using the SEQUEST search algorithm matching against the 2-27-2014 version of the Universal Protein Resoure's (UniProt) *Saccharomyces cerevisiae* database to establish protein identities. The following search parameters were used: precursor mass tolerance = 1.4 dalton, fragment mass tolerance =0.8 dalton, 2 missed cleavages were permitted, enzyme specificity was set to fully tryptic, minimum peptide length = 6 amino acids, static modifications= +57 daltons on cysteine (for all digestions that included TCEP and CAM treatment), dynamic modifications = +16 daltons on methionine and +80 daltons on serine, threonine, and tyrosine. After the initial database search, the spectra were further analyzed for individual residue phosphorylation and likelihood of interaction between Rpb3 and the other identified proteins.

The PhosphoRS node was used to identify individual phosphorylation sites. The spectra were searched using Proteome Discoverer. PhosphoRS identified signal loss on specific residues indicative of phosphorylation.

Confidence scores for the protein interactions were generated using the significance analysis of interactome (SAINT) algorithm. These calculations were performed using the Contaminant Repository for Affinity Purification (CRAPome) website (www.crapome.org, Mellacheruvu, 2013) and control sets previously produced by the Mosley lab. The datasets were searched against the *S. cerevisiae* CRAPome 1.1 database to discount likely contaminants.

The results were broken into four categories based on SAINT value (SP) of each protein hit. Hits found to have SP>0.90 were considered near certain in this work, while SP=0.75 was the lower bound for high confidence interactions. Proteins scoring between SP<0.75 and SP>0.25 were considered to be inconclusive, while a score of SP≤0.25 was considered to have no conclusive evidence of interaction. Near certain and high confidence protein hits were included in the protein network. These cutoffs were selected based on previous works (Smith-Kinnaman, 2014), as well as the distribution of scores within the data set.

RESULTS

This study investigated the changes in interactions between the Pol II subunit Rpb3 and other proteins when the *RPB9* gene is deleted. Rpb3 was chosen for extraction because this protein is a core subunit of Pol II, and because Rpb3 performs a primarily structural role within the complex. Rpb9 is a nonessential subunit, but has been linked to a variety of processes involving transcription, making this protein an ideal variable to study the interaction network of Rpb3, and by extension the interactions of Pol II.

Rpb3 and its interactors were pulled down from both wild type and *rpb9Δ* cells, and were then analyzed using MudPIT. By using *rpb9Δ* cells, we can determine which interactors are specific to the Rpb9 protein as well as proteins interacting with Pol II that are potential attempts to compensate for the deletion. Pull down was accomplished using the FLAG octopeptide, as the single purification method used with this epitope tag has been shown to extract both tightly bound proteins found in stable complexes and loosely bound proteins associated with more dynamic interactions (Gavin, 2011). Spectra resulting from this MS/MS study were analyzed to establish individual peptide sequences. These sequences were analyzed using the SEQUEST algorithm to match the peptide sequences to specific proteins. The identified spectra were then analyzed using phospho-RS to determine likely points of phosphorylation, and using SAINT to determine the likelihood that the identified protein interacts with Rpb3.

Phosphorylation Analysis

First, the spectra gathered were analyzed for phosphorylation. PhosphRS was used to calculate the probability of phosphorylation for each peptide. This was accomplished by examining amino acids known to be regularly phosphorylated, primarily serine, threonine, and tyrosine for a distinct mass shift. Phosphorylation can be assumed if one of these amino acids

shows an 80 dalton mass shift. Of the phosphorylation sites identified, all were found in both the wild type and *rpb9Δ* PolII subunits. As such, there is no conclusive evidence for a unique phosphorylation pattern caused by the absence of Rpb9.

SAINT Analysis of Pol II

Identified spectra were also analyzed using the SAINT algorithm to correlate abundance of spectra with the likelihood of an interaction with the bait protein Rpb3. The resultant SAINT probabilities (SP) ranged from 0 to 1, with a score of 1 meaning an almost certain interaction. A score of 0.5 means there is a 50% probability the proteins interact and an equal probability that the protein was pulled down by chance.

Protein identifications were organized into four categories based on SP as described above in the Methods section. Identifications with SP≥0.9 are considered to have a near certain interaction. Identifications scoring between 0.9> and SP=0.75 are classified as high confidence interactions. Proteins identifications between SP<0.75 and SP>0.25 were considered to be inconclusive, while scores of SP≤0.25 are considered to have no conclusive evidence of interaction. These relatively strict thresholds were chosen to avoid false positives due to background, as hits scoring as low as SP=0.60 could reasonably be investigated if other evidence indicated a likely interaction. See Appendix 1 for the full set of SAINT scores.

No peptides matching Rpb9 were found in the *rpb9Δ* strain, confirming the deletion. It can be inferred that Rpb9 does not affect Rpb3's interaction with other members of the complex, and furthermore that Rpb9 connects to the complex as an isolated, single protein subunit (Figure 5). This is consistent with currently available structures (Sainsbury, 2013). The slight dip in the SP of Rpb12 compared to the rest of the complex also bears explaining. This result is an artifact of a bias in the SAINT algorithm. Rpb12 is only 70 amino acids, significantly shorter than

most of the subunits, but still of equal size to Rpb10 (Carles, 1991). However, Rpb12 has only one uniquely identifiable, or proteotypic, peptide, compared to Rpb10's three (Mosley, 2011). This means that fewer peptides will be identified as definitely from this protein, and therefore the SP will be lower than the actual concentration of the protein would suggest.

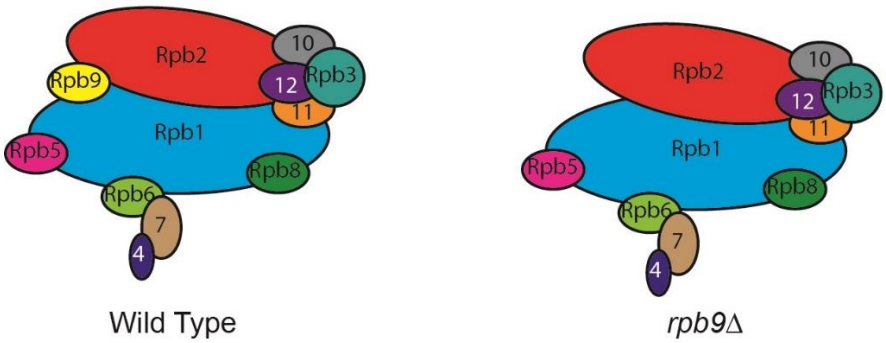

Figure 5: Schematics of Wild Type and *rpb9Δ* Pol II. Only Rpb9 is missing from the deletion strain in this dataset, implying it is an isolated subunit.

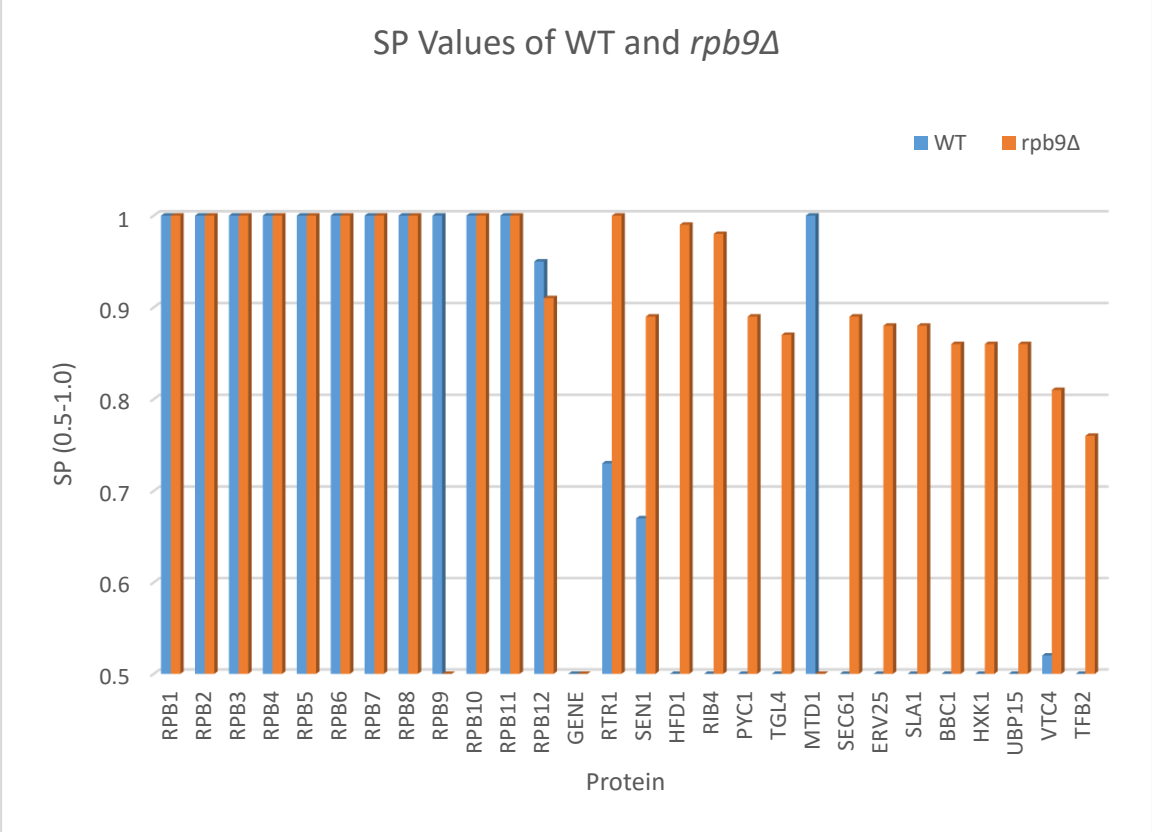

Figure 6: SP Values of WT and *rpb9Δ* strains for Pol II Subunits and Significant Hits. Fifteen protein hits not belonging to the Pol II complex were considered significant. Only Rpb9 is absent from the Pol II complex of the deletion strain, indicating a successful knockout. Also note the slightly lowered SPs of Rpb12, caused by a lack of proteolytic sequences within that protein.

Significant Hits from SAINT Analysis

Fourteen proteins were found to have a higher SP in *rpb9Δ* than in wild type. Additionally one protein, Mtd1, was shown to drop from a near certain interaction to no conclusive evidence for interaction with Rpb3 when Rpb9 was removed. A brief discussion of each of these proteins follows. Importantly, several of these proteins have no previously documented interactions with Pol II. While it is possible these hits represent novel interactions, it is also possible they were pulled down complexed to another protein. This is noted where it seems likely, based on existing literature and our dataset.

Regulator of Transcription 1 (Rtr1) scored as inconclusive (SP=0.58) in WT, but this score increased to high confidence (SP=0.75) in the *rpb9Δ* strain. Rtr1 has been shown to physically interact with Rpb3 in multiple studies (Gavin, 2006; Mosley, 2009). Interestingly, Rtr1 also appears to have a genetic interaction with Rpb9, *as rpb9* has been shown to be a high copy suppressor of *rtr1Δ* temperature sensitivity (Gibney, 2008).

Splicing Endonuclease 1 (Sen 1), an ATP-dependent RNA/DNA helicase, scored as inconclusive (SP=0.67) in WT, but scored as high confidence (SP=0.89) in *rpb9Δ*. No direct interactions between Sen1 and Rpb3 or Rpb9 have been documented. However, Sen1 has been shown to interact physically with Rpb1, the largest subunit of Pol II (Ursic, 2004). Therefore, I hypothesize that Sen1 is pulled down bound to Rpb1, and the changes witnessed were the result of altered transcription activity, rather than any specific effects that the deletion of *rpb9* has on the ability of Sen1 to complex with Rpb3.

Homolog of fatty aldehyde dehydrogenase (Hfd1) is a hexadecenal dehydrogenase. Hfd1 was not present in the WT sample (SP=0), but scored as near certain (SP=0.99) in *Δrpb9.* No physical interactions with the Pol II complex have been documented previously. It is possible,

then, that Hfd1 was pulled down due to an interaction with an accessory protein of Pol II. However, no proteins with documented interactions with both Pol II and Hfd1 were found in this dataset. It is probable that hit represents a novel interaction.

Riboflavin biosynthesis protein 4 (Rib4) is lumazine synthase. Like Hfd1, Rib4 was not present in the WT sample (SP=0), but showed a near certain interaction of SP=0.98 in *Δrpb9.* No physical interactions between Rib4 and Pol II have been documented. The most likely link between Rib4 and transcription is the protein ubiquitin specific protease 3 (Ubp3). Ubp3 has documented physical interactions with both Rib4 and the Rpb1 and Rpb2 subunits of Pol II (Kvint, 2008; Ossareh-Nazari, 2010). While Ubp3 scored as inconclusive in our dataset, Ubp3's SP score increased from SP=0.49 in WT cells to SP=0.64 in *rpb9Δ* cells. SP=0.64 is below the threshold for a high-confidence result, but is significantly above SP=0.5, and therefore an interaction between Rpb3 and Ubp3 is still possible.

Pyruvate carboxylase 1 (Pyc1) showed an increase in SP in the absence of Rpb9, going from an inconclusive result (SP=0.5) in WT cells to a high confidence score (SP=0.89) in *Δrpb9* cells. Pyc1 shows no direct interactions with the Pol II complex. In this case, the only probable link is Ess1, which has been shown to physically interact with Rpb1, Rpb2, and Rpb3 (Ho, 2002; Krogan, 2006; Ma, 2012). While Ess1 was not present in the WT samples, and has an SP of only 0.44 in *rpb9Δ* , Ess1 is the only protein with documented physical interactions to both the Pol II complex and Pyc1 present in our data set. It is possible, then, that Ess1 linked Pyc1 to Pol II during our extraction.

Triacylglycerol lipase 4 (Tgl4) was not present in the wild type sample (SP=0), but scored as high confidence (SP=0.87) in *Δrpb9*. No direct links to Pol II have been documented. Strong interactions have been documented with the cyclin dependent kinase Cdc28 and core histones

Hht1 and Hht2 (Gilmore, 2012; Ubersax, 2003). These proteins have numerous documented interactions with Pol II as well (Cosma, 2001; Chymkowitch, 2012; Smolle, 2012). However, none of these proteins had a significant presence in this dataset. This finding therefore may represent a novel interaction.

Hexokinase isoenzyme 1 (Hxk1) showed a high confidence interaction with Rpb3 only in *rpb9Δ* cells (SP=0.86), while there was no conclusive evidence for an interaction (SP=0.05) in WT cells. There are no documented interactions between Pol II and Hxk1. Two proteins in our data set, Dhh1 and Pat1, have documented interactions with Pol II and Hxk1 (Mitchell, 2013). However, Dhh1 scored SP=0.01 in WT and SP=0.22 in *rpb9Δ*, while Pat1 scored SP=0.00 in WT and SP=0.18 in *rpb9Δ*. Thus, there is then no evidence for interaction between Rpb3 and these proteins in our dataset, and Hxk1's scoring likely represents a novel interaction.

Secretory protein 61 (Sec61) scored as inconclusive in WT (SP=0.42), but scored as high confidence in *Δrpb9* (SP=0.89). There is no documentation for physical interactions between Sec61 and Pol II. She2 has been documented to interact with both Rpb1 and Sec 61 (Shen, 2010). However, in our dataset, She2 is present only in the *Δrpb9* sample, and scored as inconclusive there (SP=0.33). It is a possible link to Pol II, but it is more likely that the presence of Sec61 in our dataset represents a newly documented interaction.

ER vesicle protein 25 (Erv25) showed an increase in SP after deletion of *rpb9*, going from an inconclusive (SP=0.45) to a high confidence score (SP=0.88). There are no known physical interactions between Erv25 and Pol II. Erg5, found in this dataset, has been shown to interact with both Rpb5 and Erv25 (Tarassov, 2008). Erg5 scored inconclusively in SAINT, with WT SP=0.25 and *rpb9Δ* SP=0.44. However, it is still possible that Erv25 was pulled down bound to Erg5 and is linked to the Pol II complex through this interaction.

Sla1 show no interaction (SP=0) in WT, and a high confidence score (SP=0.88) in *Δrpb9*. Sla1 is a cytoskeletal protein binding protein. No physical interactions have been shown with Rpb3. However, Sla1 had been shown to interact physically with Sen1 (Tonikian, 2009). As mentioned above, Sen1 has documented interactions with Rpb3, and scored significantly in the *rpb9Δ* dataset.

Bbc1 showed no conclusive evidence of interaction in WT (SP=0.2), and a high confidence score in *Δrpb9* (SP=0.86). There are no documented physical interactions between Bbc1 and Pol II, and no potential links between Rpb3 and Bbc1 were found in our dataset. This hit likely indicates a novel interaction.

Ubiquitin-specific protease 15 (Ubp15) showed no interaction with Rpb3 in WT (SP=0), and a high confidence score (SP=0.86) in *Δrpb9*. Current literature shows no interactions between Ubp15 and Pol II. The protein Ssd1 has shown interactions with both Ubp15 and Rpb1 (Krogan, 2006; Phatnani, 2004). Ssd1 scored as SP=0.05 in WT and SP=0.57 in *rpb9Δ*. While this is not considered a significant hit by our criteria, it is still a possible link between Ubp15 and Rpb3.

Vacuolar transporter chaperone 4 (Vtc4) scored as inconclusive in WT (SP=0.52), and as high confidence in *Δrpb9* (SP=0.81). There are no previously documented physical interactions between Vct4 and Pol II, and no proteins present in the dataset that could act as a link between the two. It is probable this hit is a novel interaction.

Transcription factor B subunit 2 (Tfb2) is a subunit of TFIIH essential for global genomic nucleotide excision repair (Feaver, 1997). Tfb2 showed no interaction in WT (SP=0), and a high confidence score in *Δrpb9* (SP=0.76). Physical interactions have been documented between Tfb2 and Rpb7 (Duran, 2013). As a transcription factor, Tfb2 would be expected to interact with the Pol II complex.

Unlike the other protein hits, methylene tetrahydrafolate dehydrogenase (Mtd1) showed a loss of interaction with Rpb3 when Rpb9 was removed from the system, going from a near certain result (SP=1) to showing no conclusive interaction (SP=0.33). There are no previously documented physical interactions between Mtd1 and Pol II, and no proteins present in the dataset that could act as a link between the two. Therefore, this is likely a novel interaction in the WT cells. Why this has not been found in previous investigations of Rpb3 is unclear.

DISCUSSION

The interactome of Rpb3 provides a useful window for studying transcription and the function of Pol II. Rpb3 is one of the core subunits of Pol II, and interacts with a large number of proteins outside of the Pol II complex. Rpb3 is also found exclusively in Pol II, unlike several other subunits of the complex.

RPB9 was chosen for deletion because this gene encodes a non-essential subunit of Pol II, and deletion of *rpb9* has been shown to increase the rate of transcription error (Nesser, 2006). Rpb9 causes transcription to pause when a mismatched nucleotide is incorporated, both at the initial incorporation and after a second nucleotide is added. This pausing allows the proofreading mechanisms of transcription time to act on the error. The Pol II complex has shown inherent nucleotide excision activity, but this activity is enhanced by the transcription factor TFIIS. The effect of TFIIS on Pol II is reduced when the Pol II complex lacks Rpb9, in addition to the loss of pausing caused by the absence of Rpb9 (Knippa, 2013). Once the elongation complex has passed a nucleotide mismatch, it becomes much more difficult for the cell to correct the error. In many cases, transcription is simply ended prematurely, and the error-containing transcript is removed from the complex.

As detailed previously, protein hits were classified by SP. Hits with SP≥0.9 are considered to have a near certain interaction. Hits scoring 0.9>SP≥0.75 are classified as high confidence interactions. Proteins scoring 0.75>SP>0.25 were considered to be inconclusive, and hits with SP<0.25 were considered to have no evidence for interaction.

Deletion of *rpb9* caused several changes to the protein network (Figure 7). These results are not by themselves conclusive, and are offered primarily as leads for future investigations. However, suppositions can be made as to the reason for these changes in protein interactions,

and have been offered where current literature supports them. A diverse group of protein hits were produced, but broadly they can be divided by function: proteins involved transcription termination, metabolic proteins, proteins associated with transport in the Endoplasmic Reticulum, cytoskeletal proteins, proteins associated with DNA replication signaling, vacuolar transport proteins, and proteins involved with DNA repair.

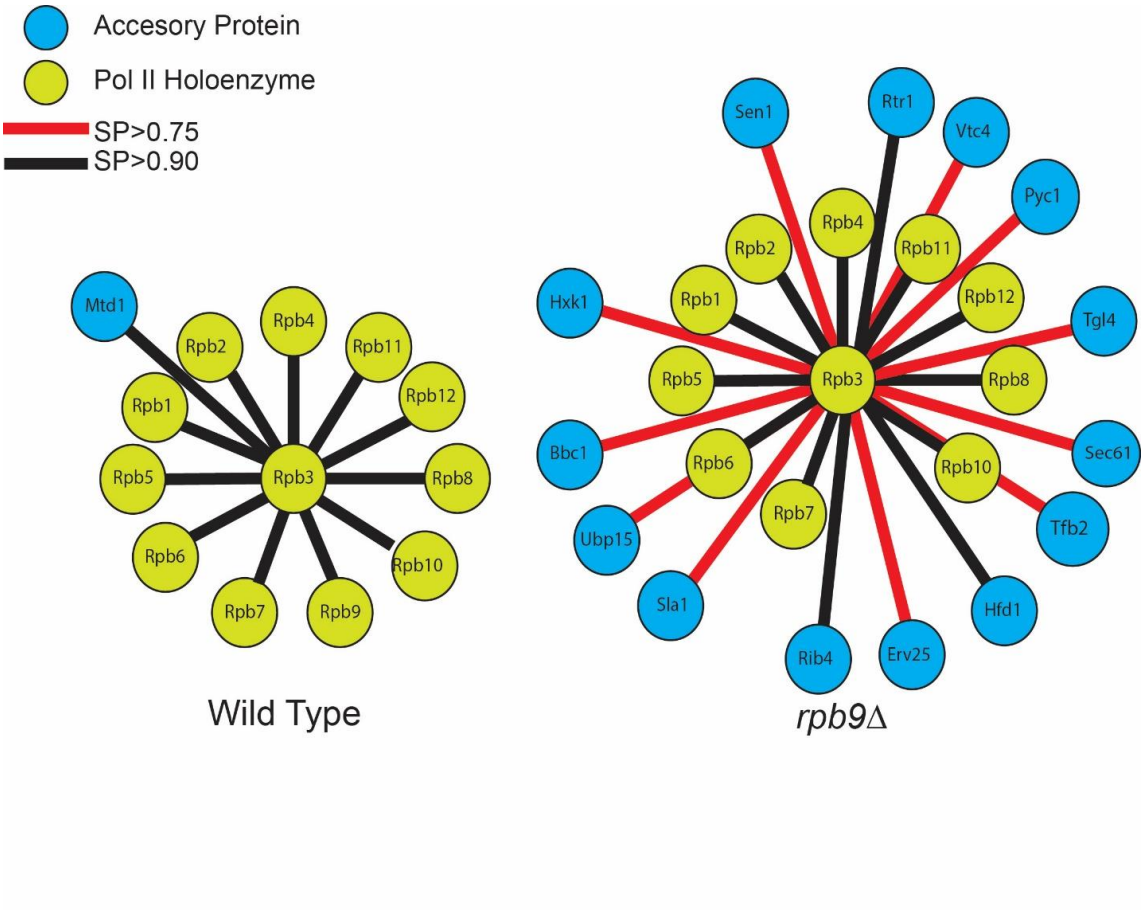

Figure 7: Changes in the Protein Network of Rpb3 between Wild Type and *rp9Δ* Cells. A number of compensations were exhibited with the deletion of RPB9.

Rtr1 and Sen1 are active in transcription elongation and Sen1 has a well described role in Pol II termination, and the presence of these two proteins is arguably the most significant result of this study. The increase in the interaction both these proteins show with Pol II after *rpb9* deletion could indicate an increased rate of transcript termination during early PolII elongation.

Rtr1 is a phosphatase that targets the CTD of Rpb1 (Mosley, 2009). The CTD region of the Pol II transcription complex is composed of a repeated heptapeptide motif with the sequence $Y_1S_2P_3T_4S_5P_6S_7$ (Corden, 1990). Modification of this region controls much of transcription. Elongation generally begins with a high level phosphorylation of the fifth serine (S5-P). As elongation continues, S5-P becomes less common, and phosphorylation of the second serine (S2-P) becomes more prevalent (Komarnitsky, 2000). CHiP studies have shown that Rtr1 is most active early in transcription (Mosley, 2009).

When *rpb9* is deleted, Rtr1's interaction score with Rpb3 increased from inconclusive in WT (SP=0.73) to near certain in *rpb9Δ* (SP=1). This change could be caused by an increased amount of early Pol II stalling during elongation, due to a loss of Rpb9's error correction activity or TCR mediation. The reverse has been previously documented, as *rpb9* overexpression has been shown to rescue the heat sensitivity of *rtr1Δ* strains (Gibney, 2008).

Sen1 is likewise important for termination and could be involved in truncation of error-containing transcripts. Sen1 is an RNA/DNA helicase that separates developing RNA strands from DNA templates, disrupting the elongation complex and terminating transcription (Porrua, 2013). This termination has been found to attenuate transcription of specific genes, notably *NRD1, HRP1,* and *IMD2*. All three of these genes share a conserved TATA box sequence, and Steinmetz (2006) has suggested that these Sen1 regulated genes may assemble a unique preinitiation complex. Sen1 interaction scores with Rpb3 increased from inconclusive (SP=0.63) to high confidence (SP=0.89) with the deletion of *rpb9.* Elevated levels of Sen1 interaction with Pol II could indicate an increased rate of transcription termination during early Pol II transcription. As mentioned above, Sen1 has been shown to interact with Rpb1 (Ursic, 2004). It

is therefore likely this result indicates an increase in the direct interaction between Rpb1 and Sen1 in the absence of Rpb9, rather than a novel interaction with Rpb3. However, it is also possible that we have identified Rpb9 as a novel regulator of Sen1 binding to Pol II.

Hfd1, Rib4, Pyc1, Tgl4, and Mtd1 are all proteins associated with the metabolism of specific molecules. Also notable is that none of these proteins have been shown to interact with the Pol II complex previously. Unique to this study, Mtd1 showed a loss of interaction after the deletion of *RPB9*. Hfd1, Rib4, Pyc1, and Tgl4 all only showed interactions in *rpb9Δ* cells.

Hfd1 showed a dramatic increase in SP in *rpb9*Δ cells compared to WT, moving from a score of no evidence of interaction (SP=0) to one of near certain interaction (SP=0.99). An aldehyde dehydrogenase, Hfd1 is involved in the breakdown of sphingosine-1-P, and is therefore crucial to the metabolism of sphingolipids (Zahedi, 2006). A defect in the human homologue of Hfd1, ALDH3A2, is responsible for Sjögren–Larsson syndrome, a rare congenital condition that causes scaly skin, neurological defects, and mild to moderate cognitive impairment (Nakahara, 2012). ALDH3A2 is also integral to the oxidative stress response, as this enzyme metabolizes aldehydes produced by reactive oxygen species (Vasiliou, 2000). It is possible Hfd1 is performing a similar role in yeast. However, the protein is found primarily on the mitochondrial membrane (Zahedi, 2006). There is little evidence for Hfd1's presence in the nucleus, and so how this protein interacts with Pol II remains obscure.

Like Hfd1, when *rpb9* was deleted Rib4's SP increased from no evidence of interaction (SP=0) to a near certain interaction (SP=0.98). Rib4 is a lumazine synthase, involved in riboflavin synthesis. Rib4 catalyzes the synthesis of 6,7-dimethyl-8-ribityllumazine, the direct precursor of riboflavin (Garcia-Ramirez, 1995). *Ashbya gossypii*, a close relative of *S. cerevisiae*, has been shown to overproduce riboflavin under stress (Schlösser, 2007). This behavior has not been

documented in wild type *S. cerevisiae*. However, as riboflavin acts as a UV protectant, it is possible this is compensation for the loss of Rpb9. Loss of Rpb9 causes increased transcription errors as well as a decrease in transcription coupled DNA repair. As such, protecting the genome from further damage due to UV light would be vital to the continued health of the organism. This model does not explain why Rib4 is found interacting with the Pol II complex.

Rib4 has no documented interactions with the Pol II complex. Rib4 has previously been shown to interact with Ubp3, a ubiquitin-specific protease that has also been shown to interact with the Rpb1 and Rpb2 subunits of Pol II (Kvint, 2008; Ossareh-Nazari, 2010). Like Rib4, Ubp3 has been shown to increase in abundance in response to DNA replication stress (Tkach, 2012). Also like Rib4, Ubp3's SP score increased in *rbp9Δ* cells (SP=0.64) as compared to WT cells (SP=0.49). It is possible that Ubp3 interacts with both the transcription machinery and Rib4 in the absence of Rpb9 as a form of compensation for the loss of transcription-coupled DNA repair, enhancing Rib4 activity in some yet undocumented way.

Pyc1 is a pyruvate carboxylase cytoplasmic enzyme that converts pyruvate to oxaloacetate (Morris, 1987). In our dataset, Pyc1 showed an inconclusive SP in WT, and a high confidence score in *rpb9Δ*. It has been shown that deletion of the gene coding Pyc1 causes no change in phenotype. However, the absence of both Pyc1 and Pyc2, another pyruvate carboxylase, prevents yeast from metabolizing glucose (Stucka, 1991). Pyc2 showed no significant interaction with Rpb3 in our data.

It is unclear why Pyc1 would interact with Rpb3 in the absence of Rpb9. There are no previously documented interactions with Rpb3, and very little in the existing literature links Pyc1 to transcription. The best model for this phenomenon involves the prolyl isomerase Ess1. Ess1 is an isomerase that acts on the CTD of Rpb1 to regulate transcription (Wu, 2000). Exx1

primarily isomerizes the Ser5-Pro6 bond of the CTD heptapeptide when Ser5 is phosphorylated (Gemmill, 2005). Such conformational changes have been shown to affect Pol II cofactor binding, and appear to also indirectly effect chromatin modification (Ma, 2012). It is possible Pyc1 is part of a feedback chain involved in this regulation, but the relationship between Pyc1 and Ess1 is not clear. Likewise, as Ess1 scored as inconclusive in our data set, it is uncertain Ess1 interacts with Pol II in the absence of Rpb9.

Tgl4 is a triacylglycerol lipase involved in metabolism of lipid particles (Athenstaedt, 2005). Tgl4 has been shown to exhibit a large range of activities, including TAG lipase, steryl ester hydrolase, phospholipase A(2) activities, and catalyzes the acyl-CoA-dependent acylation of lysophosphatidic acid to phosphatidic acid (Rajakumari, 2010). Tgl4 showed no interaction in WT, and a high confidence score in the *rp9Δ* strain. Speculation on why this protein shows a novel interaction with Rpb3 after deletion of Rpb9 is difficult. There are no documented interactions between Tgl4 and any Pol II subunit. Cdc28, a subunit of cyclin dependent kinases (CDK), has been found to interact with both Tgl4 and Rpb1. Phosphorylation of Tgl4 by Cdk1 has been shown to lead to budding during G1 phase (Kurat, 2009). This finding suggests Tgl4's interaction with Rpb3 may alter cell replication to compensate for the loss of Rpb9-related DNA repair.

Hxk1 phosphorylates glucose to begin metabolism of the sugar. Hxk1 shares this activity with hexokinase isoenzyme 2 (Hxk2), a paralog (Lobo, 1977). Hxk2 is the primary sugar hexokinase for fermentable sugars (De Winde, 1996). Hxk1, meanwhile, is most active when yeast is grown on non-fermentable carbon sources. Hxk2 has been shown to enter the nucleus to repress Hxk1 transcription, but Hxk1 has only been documented in the cytosol (Rodriguez, 2001). Hxk1 showed no evidence of interaction in the WT sample, and scored as high

confidence in *rpb9Δ*. The reason for this change in Hxk1's interaction with Rpb3 in the absence of Rpb9 remains unclear.

Both Sec61 and Erv25 are involved in transporting proteins into the endoplasmic reticulum, and show an increase in SP from an inconclusive score in WT to a high confidence score with the deletion of *rpb9*. Neither of these proteins have shown any interaction with Pol II previously. Sec61 is the largest part of a transmembrane complex called the Sec 61 complex, or translocon, located in the ER (Deshaies, 1987). In yeast, the Sec61 complex is the primary ribosomal docking port of the ER, through which proteins are translocated into the ER (Prinz, 2000). Misfolded secretory proteins are likewise transported out of the ER via this channel in competition with translocation into the ER (Kalies, 2005).

Erv25 is a member of the p24 family of vesicle coat proteins involved in ER to Golgi transport (Belden, 1996). Erv25 forms a heterotrimer with Erp1, Erp2, and Emp24 (Belden, 1996; Marzioche, 1999). However, none of these three proteins show significant interaction with Rpb3 in our dataset. Deletion of Erv25 shows a decrease in ER retention of misfolded proteins, resulting in more poorly functioning proteins being passed into the Golgi apparatus and potentially adversely affecting the cell (Copic, 2009).

The increase in interaction of both these proteins with Rpb3 in the *rpb9*Δ strain may be due to an unknown signaling network between Pol II and these transport proteins. It is possible the transcription mechanism is alerting the transport system to problems in transcription, which will result in error-containing proteins that will need to be sequestered and dismantled.

Sla1 binds to cytoskeletal proteins, and has been shown to be necessary for the formation of the cortical actin cytoskeleton (Holtzman, 1993). Deletion of *SLA1* has been shown to disrupt formation of the cortical actin cytoskeleton (Holtzman, 1993). In addition, Sla1 appears to have

an active role in endocytosis (Warren, 2002; Howard, 2002). Nuclear uptake of Sla1 is required for this function (Gardiner, 2007).

In this dataset, Sla1's SP increased from displaying no evidence of interaction to a score of high confidence. Interestingly, while Sla1 has no documented interactions with Pol II subunits, when used as a bait protein, Sla1 has pulled down Sen1 (Tonikian, 2009). Sen1, as noted previously, is a RNA/DNA helicase that has been linked to transcription termination, and also shows an increased interaction with Pol II in the absence of Rpb9. The interaction between Sla1 and Sen1 has not yet been investigated, but in the future may contribute to explaining Sla1's interactions with Rpb3 in the absence of Rpb9.

Bbc1 binds type 1 myosin (Tong, 2002). Like Sla1, Bbc1 localizes to actin patches, and appears to have a role in cytoskeletal regulation (Mochida, 2002). Deletion of the *bbc1* gene has been shown to increase the rate of endocytosis, suggesting this gene negatively regulates the process (Kaksonen, 2002). Despite having no previously documented interactions with Pol II, Bbc1 show a significant increase in interaction with Rpb3 when Rpb9 is deleted. It is possible this is due to transcription related signaling to adjust different endocytic pathways to compensate for the loss of transcription fidelity and DNA repair.

Ubp15 showed a large increase in SP, going from no interaction in WT to SP=0.89 in *Δrpb9* cells, a high confidence score. A deubiquinating protease, deletion of the gene coding for this protein has been shown to slow cell growth significantly (Amerik, 2000). This is likely due to a delay of the start of DNA replication during G2 phase caused by the deletion (Ostapenko, 2015). The interaction with Pol II may be meant to create a similar delay, to give DNA repair mechanisms additional time to compensate for the loss of Rpb9-related repair. Ubp15 has shown no previous interactions with Pol II.

Vtc4 is a vacuolar transport protein that showed an increase in interaction with Rpb3 when Rpb9 was deleted. Vtc4 is a vacuolar membrane polyphosphate polymerase and a subunit of the vacuolar transporter chaperone (VTC) complex (Chohen, 1999). Vtc4 plays a role in the fusion of vacuoles to the cell membranes (Müller, 2002). This protein has been shown to increase in abundance during DNA replication stress (Tkach, 2012). Vtc4's interaction with Pol II is likely linked to this finding, due to the loss of transcription linked DNA repair caused by the deletion of Rpb9. This is another novel interaction, as Vtc4 has no other documented interactions with Pol II.

Tfb2 interaction with Rpb3 is not present in the WT, but scored as high confidence in the absence of Rpb9. Tfb2 is a subunit of TFIIH essential for nucleotide excision repair function of TFIIH (Feaver, 1997). We found no other interaction between Rpb3 and the other TFIIH subunits in our data. Tfb2 has previously been shown to interact with Rpb7 (Duran, 2013). Tfb2 also interacts directly with Tfb5, another subunit of TFIIH (Kainov, 2010). Tfb5 has been linked to global genomic nucleotide excision repair (GG-NER), a process independent of the Rpb9-mediated transcription coupled nucleotide excision repair (TC-NER) (Ding, 2007). The novel interaction between Tfb2 with Rpb3 may be a form of up regulation of GG-NER to compensate for the loss of TC-NER due to the deletion of Rpb9.

Mtd1 is an NAD-dependent 5,10-methylenetetrahydrafolate dehydrogenase, which is a vital precursor to a number of metabolites, such as purines (West, 1993). Unlike the above proteins, deletion of Rpb9 caused a loss of a detectable interaction between Mtd1 and Rpb3, with the SP dropping from near certain to no evidence of interaction. This may be due to a change in need for nucleotides caused by altered DNA replication and transcription rates. Deletion of *rpb9* has previously been shown to cause increased sensitivity to mycophenolic acid, an inhibitor of GMP synthesis, implying there is some link between that pathway and Rpb9 (Desmoucelles, 2002).

There is a final result worth discussing. Dst1, more often referred to as TFIIS, is a transcription factor known to coregulate transcription elongation with Rpb9 (Hemming, 2000). TFIIS showed an SP of 0.69 in WT, which dropped to an SP of 0.33 in *rpb9Δ*. While both of these results are classified as "inconclusive" under this works metrics, this is due to fairly strict standards for significant hits. SP=0.69 is still a very high probability of interaction, and combined with the drop to SP=0.33 implies a definite change in TFIIS's interaction with Pol II. High-copy expression of *dst1*, the gene coding TFIIS, partially suppressed the 6-azauracil sensitivity of *rpb9Δ* (Hemming, 2000). From this we would expect to see an increase in TFIIS interaction with Pol II as a compensation for the loss of Rpb9. Instead we see the opposite. It is possible that this is due to a loss of TFIIS interaction sites within Pol II. Physical interactions between TFIIS and Rpb9 have been heavily documented, and so it is possible Rpb9 is a primary interaction point between TFIIS and Pol II (Krogan, 2006. Tarassov, 2008. Schlect, 2012). However, Rpb1, Rpb3, Rpb5, and Rpb11 have also shown interactions with TFIIS (Krogan, 2004, 2006). These subunits may allow for a reduced number interactions between Pol II and TFIIS, especially in a high-copy number environment as investigated in Hemming, et al (2000).

The classification of TFIIS as an inconclusive hit is problematic. This is a result that aligns with the current models for Rpb9 function. The classification scheme of the SAINT results in this work may be too strict, and risks wasting potentially promising hits. Moving forward, it would be worthwhile to examine our results for hits for proteins that have been associated with Rpb9, and which have SPs slightly below the "high confidence" threshold.

CONCLUSION

Pol II's transcription of mRNA is one of the most heavily studied processes in eukaryotic biochemistry. However, due to Pol II's complexity, many of the interactions between the actors in this process are still poorly understood. This work endeavored to uncover new avenues of research within this area, focusing on Rpb9's effects on the Rpb3 interactome, and by extension the entire interactome of Pol II.

These experiments generated bioinformatics hits that could be pursued in future studies. To be useful, these results would need to show both a high probability of interaction in one strain and a large change in SP between the strains. Fifteen such hits were found in this dataset. Fourteen of these showed strong interactions only in the rpb9Δ strain, while only Mtd1 was found to interact significantly with Pol II in only the WT strain. This can be attributed to the loss of Rpb9 from the Pol II complex causing a significant amount of stress the cell must compensate for, requiring the activation of additional signaling pathways.

The goal of this work was not to generate any definitive models. The pairing of MudPIT and SAINT is not a high resolution tool. This toolset is instead useful for the volume of data that it can generate and analyze. This work is a preliminary step towards a number of other studies that will expand upon the interactions discovered here.

APPENDIX 1: SAINT Table

Included below for the sake of completeness is the full table of SAINT results, listed in alphabetical order by the gene coding for the protein, and including the protein ID and SAIT scores (SP) for both the wild type and *rpb9Δ* samples.

GENE	**PROTID**	**WT SP**	***rpb9Δ* SP**	**GENE**	**PROTID**	**WT SP**	***rpb9Δ* SP**
A4UQV2	A4UQV2	0.47	0	ADH3	P07246	0.15	0.33
AAD14	P42884	0.23	0	ADH4	P10127	0	0
AAD6	P43547	0	0	ADH5	P38113	0	0.26
AAH1	P53909	0	0	ADH6	Q04894	0.03	0.33
AAP1	P37898	0.25	0.33	ADK1	P07170	0	0
AAT2	P23542	0	0	ADK2	P26364	0	0
ABD1	P32783	0	0	ADO1	P47143	0	0
ABF1	P14164	0	0	ADP1	P25371	0.47	0.31
ABF2	Q02486	0.13	0.34	ADR1	P07248	0	0.64
ABP1	P15891	0	0	ADY4	Q05955	0	0
ABP140	Q08641	0	0	AEP3	Q12089	0	0
ACC1	Q00955	0	0.07	AFG1	P32317	0	0.24
GENE	PROTID	WT SP	*rpb9Δ* SP	AFG2	P32794	0.67	0
ACH1	P32316	0	0	AFG3	P39925	0	0
ACO1	P19414	0.47	0.57	AFI1	Q99222	0	0
ACO2	P39533	0	0	AGE2	P40529	0	0
ACP1	P32463	0	0	AGP1	P25376	0	0.33
ACS2	P52910	0	0	AGP3	P43548	0	0
ACT1	P60010	0	0	AHA1	Q12449	0.03	0.29
ADD66	P36040	0	0	AHC1	Q12433	0	0
ADE1	P27616	0.08	0	AHC2	P25649	0	0
ADE12	P80210	0.85	0.62	AHP1	P38013	0.19	0.21
ADE13	Q05911	0.66	0.46	AI1	P03875	0	0
ADE16	P54113	0	0.23	AI5_BETA	Q9ZZX0	0	0
ADE17	P38009	0.36	0.31	AIF1	P52923	0	0
ADE2	P21264	0	0	AIM10	P39965	0	0
ADE3	P07245	0.25	0.33	AIM13	P43594	0	0
ADE4	P04046	0.07	0	AIM17	P23180	0	0
ADE5,7	P07244	0.72	0.33	AIM2	P39721	0	0.31
ADE6	P38972	0.42	0.1	AIM21	P40563	0	0
ADE8	P04161	0.23	0.33	AIM23	P47015	0	0
ADH1	P00330	0	0	AIM24	P47127	0	0
ADH2	P00331	0	0.33	AIM3	P38266	0	0

AIM32	Q04689	0.25	0	APN2	P38207	0	0
AIM38	P53721	0	0	APS1	P35181	0	0
AIM41	Q12032	0	0	APS3	P47064	0	0
AIM45	Q12480	0	0	APT1	P49435	0	0
AIM5	P38341	0	0	AQR1	P53943	0.25	0
AIM6	Q07716	0	0	ARA1	P38115	0	0.31
AIM9	P40053	0	0	ARB1	P40024	0	0
AIR1	P40507	0	0	ARC1	P46672	0.01	0
AKL1	P38080	0	0	ARC15	P40518	0	0
AKR1	P39010	0	0	ARC18	Q05933	0	0
ALA1	P40825	0	0	ARC19	P33204	0	0
ALB1	P47019	0	0	ARC35	P53731	0.22	0
ALD4	P46367	0	0	ARC40	P38328	0	0
ALD5	P40047	0	0	ARD1	P07347	0	0.24
ALD6	P54115	0.25	0.05	ARE2	P53629	0	0
ALE1	Q08548	0	0	ARF1	P11076	0	0
ALG11	P53954	0	0	ARF2	P19146	0	0
ALG12	P53730	0	0	ARF3	P40994	0	0.31
ALG2	P43636	0	0.33	ARG2	P40360	0	0.31
ALG5	P40350	0	0	ARG5,6	Q01217	0	0
ALG9	P53868	0.23	0	ARG7	Q04728	0	0
ALO1	P54783	0	0	ARG81	P05085	0	0
ALR1	Q08269	0	0	ARI1	P53111	0.38	0.47
ALR2	P43553	0	0	ARL1	P38116	0.11	0
ALT1	P52893	0	0	ARO1	P08566	0.78	0.87
ALY1	P36117	0.23	0	ARO10	Q06408	0	0.07
ALY2	P47029	0	0	ARO2	P28777	0	0
AMD1	P15274	0	0.03	ARO3	P14843	0	0
AMS1	P22855	0	0	ARO4	P32449	0	0
ANB1	P19211	0	0.35	ARO7	P32178	0	0
ANP1	P32629	0.24	0.3	ARO8	P53090	0	0
APA1	P16550	0.04	0.06	ARO80	Q04052	0	0
APA2	P22108	0	0	ARO9	P38840	0.03	0.31
APC1	P53886	0.25	0	ARP1	P38696	0	0
APC2	Q12440	0.25	0	ARP2	P32381	0.24	0.26
APC4	Q04601	0	0	ARP3	P47117	0	0.13
APD1	P38281	0	0.48	ARP4	P80428	0	0
APE2	P32454	0	0	ARP5	P53946	0	0.31
APE3	P37302	0	0	ARP7	Q12406	0	0
APL5	Q08951	0.42	0	ARP8	Q12386	0	0
APL6	P46682	0	0	ARR2	Q06597	0	0
APM3	P38153	0	0	ARX1	Q03862	0	0
APM4	Q99186	0	0	ASC1	P38011	0	0

ASG1	P40467	0	0	BAT2	P47176	0	0.03
ASI3	P53983	0	0	BBC1	P47068	0.2	0.86
ASK1	P35734	0	0	BCH1	Q05029	0	0.24
ASM4	Q05166	0	0	BCK1	Q01389	0	0
ASN1	P49089	0	0	BCP1	Q06338	0	0
ASN2	P49090	0.23	0	BCY1	P07278	0	0
ASP1	P38986	0	0	BDF1	P35817	0	0
ASR1	Q06834	0.49	0	BDH1	P39714	0	0.33
AST1	P35183	0	0	BEM2	P39960	0	0
ATE1	P16639	0	0	BEM3	P32873	0	0
ATF1	P40353	0	0	BET1	P22804	0	0
ATF2	P53296	0	0	BET3	P36149	0	0
ATG20	Q07528	0.42	0	BFR1	P38934	0	0
ATG21	Q02887	0	0	BFR2	Q06631	0	0
ATG27	P46989	0	0	BGL2	P15703	0	0
ATG33	Q06485	0	0.33	BI4	P03879	0	0
ATG9	Q12142	0	0	BIM1	P40013	0.18	0
ATH1	P48016	0	0	BIT2	P38346	0.25	0
ATM1	P40416	0	0	BLM10	P43583	0.18	0
ATP1	P07251	0	0	BMH1	P29311	0	0
ATP10	P18496	0	0	BMH2	P34730	0	0
ATP11	P32453	0	0	BMS1	Q08965	0	0
ATP12	P22135	0	0	BNA1	P47096	0	0
ATP14	Q12349	0	0	BNA2	P47125	0	0.31
ATP15	P21306	0	0	BNA3	P47039	0.15	0.35
ATP16	Q12165	0.23	0.33	BNA4	P38169	0	0
ATP17	Q06405	0	0.31	BNI1	P41832	0	0
ATP18	P81450	0	0	BNI4	P53858	0	0
ATP2	P00830	0	0	BNI5	P53890	0	0
ATP20	Q12233	0	0	BPT1	P14772	0	0
ATP3	P38077	0	0	BRE1	Q07457	0	0
ATP4	P05626	0	0.03	BRE4	Q07660	0	0
ATP5	P09457	0.14	0.15	BRE5	P53741	0	0
ATP7	P30902	0	0.23	BRO1	P48582	0	0
AUS1	Q08409	0	0	BRX1	Q08235	0.29	0.31
AVO1	Q08236	0	0	BSC6	Q08280	0	0
AVO2	Q04749	0	0	BUB3	P26449	0	0
AVT3	P36062	0	0	BUD20	Q08004	0	0
AVT7	P40501	0	0	BUD22	Q04347	0	0
AXL1	P40851	0	0	BUD23	P25627	0	0
AYR1	P40471	0.33	0.68	BUD6	P41697	0	0
AZF1	P41696	0	0	BUL1	P48524	0	0
BAT1	P38891	0	0	BUL2	Q03758	0.21	0

BUR6	P40096	0	0	CDC11	P32458	0.42	0.33
BZZ1	P38822	0	0	CDC12	P32468	0	0
CAB2	P40506	0.07	0	CDC123	Q05791	0	0
CAB4	P53332	0	0	CDC14	Q00684	0	0
CAB5	Q03941	0	0	CDC16	P09798	0	0
CAF120	P53836	0	0	CDC19	P00549	0	0.02
CAF20	P12962	0	0	CDC24	P11433	0	0
CAF40	P53829	0.23	0	CDC25	P04821	0	0
CAJ1	P39101	0	0	CDC26	P14724	0	0
CAM1	P29547	0	0.19	CDC27	P38042	0.23	0
CAN1	P04817	0	0.31	CDC28	P00546	0	0
CAP1	P28495	0.14	0	CDC3	P32457	0	0
CAP2	P13517	0	0	CDC31	P06704	0	0
CAR1	P00812	0	0	CDC33	P07260	0	0.01
CAR2	P07991	0.57	0.33	CDC34	P14682	0	0
CAT5	P41735	0	0	CDC36	P06100	0	0
CAT8	P39113	0	0	CDC37	P06101	0	0
CBF1	P17106	0	0	CDC39	P25655	0.15	0.31
CBF2	P32504	0	0	CDC42	P19073	0.24	0.01
CBF5	P33322	0.25	0.33	CDC48	P25694	0	0
CBK1	P53894	0	0	CDC50	P25656	0	0.31
CBP6	P07253	0	0	CDC53	Q12018	0.22	0.33
CBR1	P38626	0.03	0.34	CDC55	Q00362	0	0.23
CBS2	P14905	0	0	CDC60	P26637	0	0
CBT1	P36038	0	0	CDC73	Q06697	0	0.23
CCA1	P21269	0	0	CDC9	P04819	0	0.33
CCC1	P47818	0	0	CDS1	P38221	0	0.18
CCH1	P50077	0	0.33	CEF1	Q03654	0.23	0
CCL1	P37366	0	0	CEG1	Q01159	0	0.14
CCP1	P00431	0	0.33	CEP3	P40969	0	0
CCR4	P31384	0	0	CET1	O13297	0.31	0
CCS1	P40202	0.02	0.08	CEX1	Q12453	0.25	0.31
CCT2	P39076	0	0	CFT1	Q06632	0	0
CCT3	P39077	0.22	0.13	CHA1	P25379	0	0.32
CCT4	P39078	0.24	0.59	CHC1	P22137	0	0.6
CCT5	P40413	0	0.67	CHD1	P32657	0.23	0
CCT6	P39079	0	0	CHK1	P38147	0.23	0
CCT7	P42943	0.02	0	CHL1	P22516	0	0
CCT8	P47079	0	0.31	CHL4	P38907	0	0
CCZ1	P38273	0	0	CHO2	P05374	0.5	0.64
CDA2	Q06703	0	0	CHS1	P08004	0	0.07
CDC1	P40986	0.25	0	CHS2	P14180	0	0
CDC10	P25342	0.23	0.15	CHS3	P29465	0	0

CHS5	Q12114	0	0	COX6	P00427	0	0.03
CIC1	P38779	0	0	COY1	P34237	0.25	0
CIK1	Q01649	0	0	CPA1	P07258	0	0
CIN1	P40987	0	0	CPA2	P03965	0	0
CIR1	P42940	0	0.01	CPR1	P14832	0.5	0.32
CIR2	Q08822	0	0	CPR3	P25719	0	0
CIS3	P47001	0	0	CPR4	P25334	0	0
CIT1	P00890	0	0.58	CPR5	P35176	0.67	0
CKA1	P15790	0.01	0.2	CPR6	P53691	0.02	0
CKA2	P19454	0.27	0.64	CPR8	P53728	0	0
CKB1	P43639	0	0.03	CPS1	P27614	0.01	0.52
CKB2	P38930	0	0	CRC1	Q12289	0	0
CKI1	P20485	0.25	0	CRM1	P30822	0.02	0.33
CKS1	P20486	0	0	CRN1	Q06440	0	0
CLB2	P24869	0	0	CRP1	P38845	0	0
CLC1	P17891	0	0	CRT10	Q08226	0	0
CLF1	Q12309	0	0	CSE1	P33307	0.4	0.3
CLU1	Q03690	0	0	CSE2	P33308	0	0
CMD1	P06787	0	0.03	CSF1	Q12150	0	0
CMK2	P22517	0	0	CSL4	P53859	0	0
CMP2	P14747	0	0	CSM1	P25651	0	0
CMS1	Q07897	0	0	CSR1	Q06705	0	0
CNA1	P23287	0	0.18	CSR2	Q12734	0	0
CNB1	P25296	0	0	CST26	P38226	0	0.31
CNS1	P33313	0	0	CTF18	P49956	0.41	0
COF1	Q03048	0	0	CTF3	Q12748	0	0
COG2	P53271	0	0	CTF4	Q01454	0	0
COG3	P40094	0	0	CTF8	P38877	0	0
COG5	P53951	0	0	CTI6	Q08923	0	0
COG6	P53959	0	0.56	CTL1	Q03220	0	0
COG7	P53195	0	0	CTR9	P89105	0	0
COP1	P53622	0.08	0	CTT1	P06115	0	0
COQ1	P18900	0	0.65	CUE5	Q08412	0	0
COQ5	P49017	0	0	CUL3	P53202	0.23	0
COQ6	P53318	0	0.24	CWH41	P53008	0.18	0.24
COQ8	P27697	0	0	CWH43	P25618	0.1	0.04
COR1	P07256	0.02	0.17	CYC1	P00044	0.4	0.47
COT1	P32798	0.25	0	CYC2	P38909	0	0
COX10	P21592	0	0	CYC7	P00045	0	0.33
COX13	P32799	0	0	CYC8	P14922	0	0.57
COX15	P40086	0	0.33	CYM1	P32898	0.18	0
COX18	P53239	0	0	CYR1	P08678	0	0
COX4	P04037	0	0	CYS3	P31373	0.02	0.01

CYS4	P32582	0	0.33	DNF1	P32660	0	0.32
CYT1	P07143	0	0	DNF2	Q12675	0	0
DAD3	P69850	0	0	DNF3	Q12674	0	0
DAK1	P54838	0	0	DNL4	Q08387	0	0
DAL7	P21826	0	0	DNM1	P54861	0.34	0.3
DAP1	Q12091	0	0	DOC1	P53068	0.4	0
DAS1	P47005	0.58	0	DOM34	P33309	0	0
DBF2	P22204	0	0	DOP1	Q03921	0.41	0.45
DBP2	P24783	0	0	DOS2	P54858	0	0
DBP3	P20447	0	0.02	DOT5	P40553	0	0
DBP5	P20449	0.21	0	DOT6	P40059	0	0
DBP6	P53734	0	0	DPB11	P47027	0	0
DBP9	Q06218	0	0.33	DPB2	P24482	0	0
DCP1	Q12517	0	0	DPB4	Q04603	0	0
DCS1	Q06151	0.23	0.15	DPH2	P32461	0.23	0
DDI2;DDI3	P0CH63	0	0	DPH5	P32469	0	0
DDP1	Q99321	0.04	0.33	DPL1	Q05567	0	0.65
DDR48	P18899	0	0	DPM1	P14020	0.41	0
DED1	P06634	0	0	DPP1	Q05521	0	0.31
DED81	P38707	0	0	DPS1	P04802	0	0
DEF1	P35732	0.25	0	DRE2	P36152	0	0
DEG1	P31115	0	0.31	DRS2	P39524	0	0.44
DEP1	P31385	0	0	DSE3	Q08729	0	0
DET1	Q99288	0	0	DSF1;YNR073C	P0CX08	0	0
DFG5	Q05031	0	0	DSK2	P48510	0	0
DFM1	Q12743	0.12	0.15	DSS4	P32601	0.25	0
DHH1	P39517	0.01	0.22	DST1	P07273	0.69	0.33
DIA3	P52290	0	0	DUG1	P43616	0	0
DID2	P69771	0	0	DUG2	P38149	0	0
DID4	P36108	0	0	DUG3	P53871	0	0
DIG1	Q03063	0	0	DUN1	P39009	0	0
DIM1	P41819	0	0	DUO1	P53168	0	0
DIP2	Q12220	0.57	0	DUR1,2	P32528	0.5	0.67
DIP5	P53388	0.23	0.33	DUS3	Q06053	0	0
DIS3	Q08162	0	0	DYN1	P36022	0.26	0
DIT1	P21623	0	0	DYN2	Q02647	0	0
DJP1	P40564	0	0	DYS1	P38791	0	0
DLD3	P39976	0.16	0.18	E2QC18	E2QC18	0	0
DLT1	Q04216	0	0	E9PAE3	E9PAE3	0	0
DMA1	P38823	0.25	0	EAF1	Q06337	0	0
DMA2	P53924	0	0.15	EAF3	Q12432	0	0
DMC1	P25453	0.48	0	EAF5	P39995	0	0
DNA2	P38859	0	0.31	EAF7	P53911	0	0.33

EAP1	P36041	0	0	END3	P39013	0	0
EAR1	Q03212	0	0	ENO1	P00924	0.24	0.33
EBP2	P36049	0	0.26	ENO2	P00925	0	0
EBS1	Q03466	0	0	ENP1	P38333	0.21	0.05
ECM1	P39715	0	0	ENP2	P48234	0	0
ECM10	P39987	0	0.33	ENT1	Q12518	0	0
ECM16	Q04217	0	0	ENT3	P47160	0	0
ECM19	Q06011	0	0	ENV11	P53246	0	0
ECM2	P38241	0	0	ENV7	Q12003	0	0
ECM21	P38167	0	0	EPS1	P40557	0	0
ECM25	P32525	0.48	0.33	ERB1	Q04660	0	0
ECM29	P38737	0.55	0.23	ERG1	P32476	0	0.53
ECM3	Q99252	0	0	ERG10	P41338	0	0.17
ECM30	Q06673	0	0	ERG11	P10614	0	0.17
ECM32	P32644	0	0.33	ERG12	P07277	0.42	0
ECM33	P38248	0	0	ERG13	P54839	0.47	0.49
ECM4	P36156	0	0	ERG2	P32352	0	0
EDC3	P39998	0	0	ERG20	P08524	0.06	0
EDE1	P34216	0	0	ERG25	P53045	0	0.31
EFB1	P32471	0.04	0	ERG26	P53199	0	0.23
EFG1	Q3E705	0	0	ERG27	Q12452	0	0.35
EFM1	P38732	0	0	ERG28	P40030	0.26	0.44
EFR3	Q03653	0	0	ERG3	P32353	0.18	0
EFT1;EFT2	P32324	0	0	ERG4	P25340	0.23	0.31
EGD1	Q02642	0.05	0	ERG5	P54781	0.25	0.44
EGD2	P38879	0	0	ERG6	P25087	0	0.14
EHD3	P28817	0	0	ERG7	P38604	0	0
EHT1	P38295	0	0	ERG8	P24521	0	0
EIS1	Q05050	0	0	ERG9	P29704	0.46	0.33
ELA1	P53861	0	0	ERJ5	P43613	0	0.33
ELO1	P39540	0	0	ERO1	Q03103	0	0
ELP2	P42935	0	0	ERP1	Q05359	0	0.07
ELP3	Q02908	0	0	ERP2	P39704	0	0.33
EMC1	P25574	0	0.24	ERP3	Q12403	0	0
EMC2	P47133	0	0	ERP4	Q12450	0	0
EMC4	P53073	0	0	ERV1	P27882	0	0
EMG1	Q06287	0.05	0	ERV14	P53173	0.47	0.31
EMI1	Q04406	0	0	ERV2	Q12284	0	0
EMP24	P32803	0	0.29	ERV25	P54837	0.45	0.88
EMP47	P43555	0	0.14	ERV29	P53337	0	0.15
EMP70	P32802	0	0.14	ERV41	Q04651	0.18	0
EMW1	P42842	0.18	0.33	ERV46	P39727	0	0.33
ENA1	P13587	0	0.21	ESC1	Q03661	0	0

ESF2	P53743	0	0	FMP43	P53311	0	0
ESP1	Q03018	0	0	FMP52	P40008	0	0
ESS1	P22696	0	0.44	FOL1	P53848	0	0
ETR1	P38071	0.18	0	FOL2	P51601	0.47	0.3
ETT1	Q08421	0.21	0.14	FPR1	P20081	0	0
EXG2	P52911	0	0	FPR2	P32472	0	0
EXO84	P38261	0	0	FPR3	P38911	0.24	0.53
FAA1	P30624	0.25	0.64	FPR4	Q06205	0.14	0.11
FAA2	P39518	0	0	FPS1	P23900	0	0
FAA3	P39002	0.5	0	FRA1	Q07825	0	0
FAA4	P47912	0.01	0.11	FRE1	P32791	0	0
FAB1	P34756	0	0.31	FRE4	P53746	0	0
FAD1	P38913	0	0	FRK1	Q03002	0	0
FAF1	P40546	0	0	FRQ1	Q06389	0	0
FAL1	Q12099	0	0	FRS1	P15624	0.11	0.02
FAP1	P53971	0	0	FRS2	P15625	0	0
FAP7	Q12055	0	0	FRT1	Q99332	0	0
FAR11	P53917	0	0	FTR1	P40088	0.5	0
FAR3	P46671	0	0	FUM1	P08417	0.5	0.27
FAR8	Q05040	0	0	FUN12	P39730	0	0
FAS1	P07149	0	0.67	FUN14	P18411	0	0
FAS2	P19097	0	0.28	FUN19	P28003	0	0.31
FAT1	P38225	0.18	0.33	FUN26	P31381	0.4	0
FAU1	P40099	0	0.31	FUN30	P31380	0	0
FBA1	P14540	0	0.01	FUR1	P18562	0	0
FBP26	P32604	0	0	FUR4	P05316	0	0
FCJ1	P36112	0	0.3	FUS3	P16892	0	0
FCY2	P17064	0.23	0.23	GAA1	P39012	0	0
FCY22	Q12119	0	0	GAL1	P04385	0	0
FEN1	P25358	0.18	0	GAL11	P19659	0	0
FES1	P38260	0	0	GAL4	P04386	0	0
FET3	P38993	0.23	0.33	GAL83	Q04739	0.25	0
FET4	P40988	0.69	0.33	GAP1	P19145	0	0.33
FET5	P43561	0	0	GAR1	P28007	0	0.03
FIP1	P45976	0	0	GAS1	P22146	0	0
FIS1	P40515	0	0	GAS3	Q03655	0	0
FKH2	P41813	0	0	GAS5	Q08193	0	0
FKS1	P38631	0	0.33	GBP2	P25555	0.23	0
FKS3	Q04952	0	0	GCD1	P09032	0	0
FLC3	P53121	0	0	GCD11	P32481	0	0
FLO1	P32768	0	0	GCD2	P12754	0	0
FLO9	P39712	0	0	GCD6	P32501	0.18	0
FMP27	Q06179	0.25	0	GCD7	P32502	0	0.31

GCN1	P33892	0.26	0.36	GLO4	Q12320	0	0
GCN20	P43535	0.25	0.33	GLR1	P41921	0	0
GCN3	P14741	0.48	0.67	GLT1	Q12680	0	0
GCN5	Q03330	0	0	GLY1	P37303	0	0
GCS1	P35197	0	0	GND1	P38720	0.17	0.31
GCV1	P48015	0.48	0	GNP1	P48813	0	0.23
GCV2	P49095	0.26	0	GNT1	Q12096	0	0
GCV3	P39726	0.33	0.33	GOS1	P38736	0	0
GDA1	P32621	0.06	0.47	GOT1	Q03554	0	0
GDE1	Q02979	0	0	GPA1	P08539	0	0
GDH1	P07262	0	0	GPA2	P10823	0	0
GDI1	P39958	0.21	0.12	GPB1	Q08886	0	0
GEA1	P47102	0	0.33	GPD1	Q00055	0	0.33
GEA2	P39993	0	0.33	GPD2	P41911	0.1	0.26
GEF1	P37020	0	0	GPH1	P06738	0	0.33
GEM1	P39722	0	0	GPI13	Q07830	0	0
GET1	P53192	0	0	GPI16	P38875	0.23	0
GET2	P40056	0	0	GPM1	P00950	0	0
GET3	Q12154	0	0.33	GPT2	P36148	0	0
GET4	Q12125	0	0.38	GRH1	Q04410	0	0
GFA1	P14742	0.17	0.33	GRS1	P38088	0	0
GFD2	P25370	0	0	GRS2	Q06817	0.25	0
GGA1	Q06336	0.05	0.2	GRX1	P25373	0.23	0.54
GGA2	P38817	0.46	0.32	GRX2	P17695	0.06	0
GGC1	P38988	0	0	GRX3	Q03835	0	0
GID7	P25569	0.42	0.31	GRX4	P32642	0	0.31
GIM3	P53900	0	0	GRX5	Q02784	0	0.14
GIM4	P40005	0	0	GRX7	P38068	0	0
GIM5	Q04493	0	0	GSC2	P40989	0.49	0.34
GIP1	P38229	0	0	GSF2	Q04697	0	0
GIP4	P39732	0	0	GSH2	Q08220	0	0
GIR2	Q03768	0	0	GSP1	P32835	0	0
GIS1	Q03833	0	0	GSY1	P23337	0	0
GIS2	P53849	0.36	0	GSY2	P27472	0	0
GLC7	P32598	0	0.06	GTB1	Q04924	0	0
GLE1	Q12315	0	0	GTO1	P48239	0	0
GLE2	P40066	0	0	GTS1	P40956	0	0
GLK1	P17709	0.18	0.65	GTT1	P40582	0	0
GLN1	P32288	0	0.01	GTT3	P39996	0	0
GLN4	P13188	0	0.02	GUA1	P38625	0	0
GLO1	P50107	0	0.33	GUF1	P46943	0.48	0
GLO2	Q05584	0	0	GUK1	P15454	0	0
GLO3	P38682	0	0	GUP1	P53154	0	0

GUS1	P46655	0	0	HIT1	P46973	0	0
GUT2	P32191	0	0	HLJ1	P48353	0	0
GVP36	P40531	0	0	HMF1	P40037	0.18	0.33
GYL1	Q04322	0	0.31	HMG1	P12683	0	0.33
GYP5	Q12344	0	0.31	HMG2	P12684	0.34	0
GYP6	P32806	0	0	HMI1	Q12039	0	0
GYP7	P48365	0	0	HMO1	Q03973	0	0
GZF3	P42944	0	0	HMRA1	P0CY11	0	0
HAL5	P38970	0	0	HMT1	P38074	0.42	0
HAP1	P0CE41	0	0	HNM1	P19807	0	0
HAS1	Q03532	0	0	HNT1	Q04344	0	0
HAT1	Q12341	0	0	HOC1	P47124	0.42	0.44
HBS1	P32769	0	0	HOG1	P32485	0.5	0.31
HCA4	P20448	0	0	HOM2	P13663	0	0
HCH1	P53834	0	0.15	HOM3	P10869	0	0
HCM1	P25364	0	0	HOM6	P31116	0	0
HCR1	Q05775	0	0	HPF1	Q05164	0	0
HDA1	P53973	0	0	HPT1	Q04178	0	0
HEF3	P53978	0	0.03	HRB1	P38922	0	0
HEH2	Q03281	0	0	HRD3	Q05787	0	0
HEK2	P38199	0.17	0.34	HRI1	Q05905	0.25	0
HEM1	P09950	0	0.33	HRP1	Q99383	0.01	0
HEM13	P11353	0	0	HRQ1	Q05549	0	0
HEM14	P40012	0	0.23	HRR25	P29295	0	0.23
HEM15	P16622	0	0.08	HSC82	P15108	0	0
HEM2	P05373	0.25	0	HSF1	P10961	0	0
HEM3	P28789	0	0	HSK3	P69852	0	0
HER1	Q12276	0	0	HSL7	P38274	0.05	0
HFA1	P32874	0.4	0.33	HSM3	P38348	0	0
HFD1	Q04458	0	0.99	HSP10	P38910	0	0
HGH1	P48362	0	0	HSP104	P31539	0	0.08
HHF1;HHF2	P02309	0	0.2	HSP12	P22943	0	0
HHO1	P53551	0	0	HSP26	P15992	0	0.49
HHT1;HHT2	P61830	0.04	0.11	HSP30	P25619	0	0.33
HIF1	Q12373	0	0	HSP42	Q12329	0.73	0.78
HIM1	Q06674	0	0	HSP60	P19882	0	0
HIP1	P06775	0	0	HSP78	P33416	0	0.08
HIR2	P32480	0	0	HSP82	P02829	0	0
HIR3	P47171	0	0	HST2	P53686	0	0
HIS1	P00498	0	0	HST3	P53687	0	0
HIS4	P00815	0.55	0.47	HSV2	P50079	0	0
HIS5	P07172	0	0	HTA1	P04911	0.49	0.62
HIS7	P33734	0	0	HTB1	P02293	0	0

HTL1	Q9URQ5	0	0	IMG2	P25642	0	0
HTS1	P07263	0	0.03	IMH1	Q06704	0	0
HTZ1	Q12692	0	0	IML1	P47170	0	0
HUL5	P53119	0	0	IML2	P47031	0	0
HXK1	P04806	0.05	0.86	IML3	P38265	0	0
HXK2	P04807	0	0	IMP2	P32351	0	0
HXT2	P23585	0	0	IMP3	P32899	0	0.31
HXT3	P32466	0	0.33	IMP4	P53941	0	0
HXT4	P32467	0	0.33	INM2	Q05533	0	0
HXT5	P38695	0	0	INN1	P53901	0	0
HXT6	P39003	0.17	0.31	INO4	P13902	0	0
HXT7	P39004	0	0.67	INO80	P53115	0	0
HYM1	P32464	0	0	INP2	Q03824	0	0
HYP2	P23301	0	0.32	INP51	P40559	0	0
HYR1	P40581	0	0	INP52	P50942	0	0
ICP55	P40051	0	0	INP53	Q12271	0	0
ICY1	Q04329	0	0	IOC4	Q04213	0	0
IDH1	P28834	0.03	0.33	IPI3	P53877	0	0
IDH2	P28241	0.31	0.33	IPP1	P00817	0.02	0
IDI1	P15496	0	0	IPT1	P38954	0	0
IDP1	P21954	0.25	0.65	IRA1	P18963	0	0
IDP2	P41939	0	0	IRA2	P19158	0.25	0
IDS2	P46958	0	0	IRC14	Q08522	0	0
IES1	P43579	0	0	IRC18	P47056	0	0
IES3	Q12345	0	0	IRC19	Q07843	0	0
IES4	Q08561	0	0	IRC20	Q06554	0	0
IFA38	P38286	0.17	0	IRC21	Q04772	0	0
IFH1	P39520	0	0	IRC24	P40580	0.09	0
IFM1	P25038	0	0	IRC5	P43610	0	0
IGO1	P53897	0	0	IRC8	P47046	0	0
IKI3	Q06706	0.14	0.19	ISA2	Q12425	0	0
ILS1	P09436	0	0.32	ISC1	P40015	0	0
ILV1	P00927	0	0.04	ISD11	Q6Q560	0	0
ILV2	P07342	0	0	ISR1	Q06098	0	0
ILV3	P39522	0	0	IST1	P53843	0	0
ILV5	P06168	0.25	0	IST2	P38250	0.03	0.21
ILV6	P25605	0	0	IST3	P40565	0	0
IMD1	P39567	0	0	ISU1	Q03020	0	0
IMD2	P38697	0	0	ISW1	P38144	0	0.33
IMD3	P50095	0	0	ISW2	Q08773	0.18	0
IMD4	P50094	0	0	ITR1	P30605	0	0
IME1	P21190	0	0	IVY1	Q04934	0	0
IMG1	P25626	0	0	IWR1	Q07532	0.4	0

IZH2	Q12442	0	0	KTR1	P27810	0	0.01
JIP4	Q03361	0	0	KTR2	P33550	0	0
JIP5	Q06214	0	0	KTR3	P38130	0.01	0
JJJ3	P47138	0	0	KTR4	P38131	0.17	0.15
JNM1	P36224	0	0	KXD1	P53158	0	0
JSN1	P47135	0	0	LAA1	P39526	0	0
KAE1	P36132	0.23	0	LAP2	Q10740	0	0
KAP104	P38217	0.48	0	LAP4	P14904	0.26	0
KAP120	Q02932	0.43	0.31	LAS17	Q12446	0.23	0
KAP122	P32767	0	0.33	LAS21	P40367	0	0
KAP123	P40069	0.01	0.33	LAT1	P12695	0	0.32
KAP95	Q06142	0.06	0.5	LCB1	P25045	0.22	0.18
KAR2	P16474	0	0	LCB2	P40970	0	0.15
KAR9	P32526	0.23	0	LCB4	Q12246	0	0
KCC4	P25389	0	0	LCD1	Q04377	0	0
KCS1	Q12494	0	0.55	LCL2	Q08045	0	0
KEL1	P38853	0	0	LCP5	P40079	0	0
KEL3	Q08979	0	0	LDH1	P38139	0	0.31
KES1	P35844	0.41	0.28	LEM3	P42838	0	0
KEX1	P09620	0	0.14	LEO1	P38439	0	0.31
KEX2	P13134	0	0.31	LEU1	P07264	0	0
KGD1	P20967	0.28	0.66	LEU4	P06208	0.01	0
KGD2	P19262	0	0.64	LGE1	Q02796	0	0
KIC1	P38692	0	0	LHP1	P33399	0	0
KIN1	P13185	0.4	0	LHS1	P36016	0	0
KIN2	P13186	0	0	LIA1	P47120	0	0.02
KIN28	P06242	0	0	LIF1	P53150	0	0
KIN3	P22209	0	0	LIP5	P32875	0	0
KIP1	P28742	0.58	0	LOC1	P43586	0	0
KIP2	P28743	0	0	LOS1	P33418	0	0
KIP3	P53086	0	0	LOT5	P34234	0	0
KNS1	P32350	0	0	LPD1	P09624	0	0.02
KOG1	P38873	0.65	0	LRO1	P40345	0	0
KRE2	P27809	0.43	0.68	LRP1	P38801	0	0
KRE27	P40540	0	0.31	LSB3	P43603	0.09	0.32
KRE33	P53914	0.17	0.42	LSB5	P25369	0	0
KRE5	P22023	0	0	LSC1	P53598	0	0
KRE6	P32486	0	0	LSC2	P53312	0	0
KRR1	P25586	0	0	LSG1	P53145	0	0
KRS1	P15180	0	0	LSM1	P47017	0	0
KSP1	P38691	0	0.33	LSM2	P38203	0	0
KSS1	P14681	0.21	0	LSM4	P40070	0	0
KTI12	P34253	0.04	0	LSM5	P40089	0	0

LSM6	Q06406	0	0	MDL1	P33310	0	0.54
LSP1	Q12230	0	0	MDM1	Q01846	0	0
LST4	P34239	0	0	MDM12	Q92328	0	0.31
LST8	P41318	0	0	MDM20	Q12387	0	0.14
LUC7	Q07508	0	0	MDM32	Q12171	0	0.31
LYP1	P32487	0	0.33	MDM35	O60200	0	0
LYS1	P38998	0.32	0.55	MDM36	Q06820	0	0
LYS12	P40495	0	0	MDM38	Q08179	0	0.33
LYS2	P07702	0.49	0	MDN1	Q12019	0.44	0.28
LYS20	P48570	0	0	MDR1	P53258	0	0
LYS21	Q12122	0	0	MDY2	Q12285	0	0
LYS9	P38999	0	0.56	MEC1	P38111	0	0
MAD1	P40957	0	0.33	MED2	Q12124	0	0
MAD3	P47074	0	0	MED6	P38782	0	0
MAE1	P36013	0.25	0.34	MED8	P38304	0	0
MAK21	Q12176	0	0	MES1	P00958	0	0
MAK3	Q03503	0	0	MET10	P39692	0	0
MAK31	P23059	0	0	MET12	P46151	0	0
MAK5	P38112	0.23	0	MET13	P53128	0	0
MAL11	P53048	0.48	0.54	MET18	P40469	0	0.14
MAM33	P40513	0	0	MET32	Q12041	0	0
MAP1	Q01662	0.24	0.14	MET5	P47169	0	0
MAP2	P38174	0.11	0	MET6	P05694	0.61	0
MAS2	P11914	0	0	MET7	Q08645	0	0
MBF1	O14467	0	0	MEU1	Q07938	0.15	0
MBP1	P39678	0	0	MEX67	Q99257	0	0
MCA1	Q08601	0	0	MFT1	P33441	0	0
MCD1	Q12158	0	0	MGE1	P38523	0	0
MCD4	P36051	0	0	MGM1	P32266	0	0
MCH5	Q08777	0	0	MGM101	P32787	0.06	0.33
MCK1	P21965	0.45	0.38	MGR1	P25573	0	0
MCM2	P29469	0	0	MGR3	Q04472	0	0
MCM22	P47167	0	0	MHR1	Q06630	0	0
MCM3	P24279	0	0	MIA40	P36046	0	0
MCM4	P30665	0	0.01	MID2	P36027	0	0
MCM5	P29496	0	0	MIP1	P15801	0	0
MCM6	P53091	0	0	MIR1	P23641	0.21	0.22
MCM7	P38132	0	0.23	MIS1	P09440	0.3	0.31
MCR1	P36060	0	0	MKC7	P53379	0	0
MCX1	P38323	0	0.33	MKT1	P40850	0.25	0
MDE1	P47095	0	0	MLC1	P53141	0	0
MDH3	P32419	0	0.31	MLC2	Q06580	0	0
MDJ1	P35191	0.26	0.33	MLF3	P32047	0	0

MLP1	Q02455	0	0.06	MRPL32	P25348	0	0
MLP2	P40457	0	0	MRPL33	P20084	0	0
MMF1	P40185	0	0	MRPL35	Q06678	0	0
MMP1	Q12372	0	0	MRPL44	P19956	0	0
MMR1	Q06324	0	0	MRPL6	P32904	0	0
MMS1	Q06211	0	0	MRPS16	Q02608	0	0
MMS22	Q06164	0	0	MRPS17	Q03246	0	0
MND1	P53102	0	0	MRPS35	P53292	0	0
MNN1	P39106	0	0	MRPS5	P33759	0	0
MNN10	P50108	0	0	MRPS8	Q03799	0.66	0
MNN11	P46985	0.21	0.31	MRPS9	P38120	0	0
MNN2	P38069	0	0.01	MRS6	P32864	0	0
MNN5	P46982	0	0	MRT4	P33201	0	0
MNN9	P39107	0.04	0.45	MSA2	P36157	0	0
MNP1	P53163	0.06	0.03	MSB1	P21339	0.25	0
MOD5	P07884	0	0	MSC2	Q03455	0	0
MON2	P48563	0	0	MSC7	P38694	0	0
MOT1	P32333	0	0	MSD1	P15179	0	0
MOT2	P34909	0	0	MSE1	P48525	0.18	0
MOT3	P54785	0	0	MSF1	P08425	0	0
MPD2	Q99316	0	0	MSH1	P25846	0	0
MPM1	P40364	0	0	MSH2	P25847	0.21	0.28
MPP10	P47083	0	0	MSH4	P40965	0	0
MRD1	Q06106	0	0	MSH5	Q12175	0	0
MRH1	Q12117	0	0.26	MSH6	Q03834	0	0
MRI1	Q06489	0	0	MSM1	P22438	0	0
MRL1	Q06815	0	0	MSN4	P33749	0	0
MRN1	Q08925	0	0	MSN5	P52918	0.23	0
MRP1	P10662	0.04	0	MSP1	P28737	0	0
MRP17	P28778	0	0	MSS11	Q03825	0	0
MRP21	P38175	0	0	MSS116	P15424	0	0.08
MRP4	P32902	0	0.15	MSS51	P32335	0	0
MRP51	Q02950	0	0	MTC1	P47018	0	0
MRP8	P35719	0	0	MTC5	Q03897	0	0
MRPL10	P36520	0	0	MTD1	Q02046	1	0.33
MRPL11	P36521	0	0	MTG2	P38860	0	0
MRPL13	Q02204	0	0	MTM1	P53320	0	0
MRPL16	P38064	0	0	MTR10	Q99189	0	0
MRPL19	P53875	0	0.24	MTR3	P48240	0.4	0
MRPL22	P53881	0	0	MTR4	P47047	0.04	0
MRPL23	Q12487	0	0.31	MUB1	Q03162	0	0
MRPL27	P36526	0	0	MUM2	P38236	0	0
MRPL3	P36516	0	0	MUP1	P50276	0	0

MVP1	P40959	0	0	NHP2	P32495	0.35	0.29
MXR1	P40029	0	0	NHP6A	P11632	0	0
MYO1	P08964	0	0	NHP6B	P11633	0	0
MYO2	P19524	0.25	0.52	NIC96	P34077	0	0.01
MYO3	P36006	0	0	NIF3	P53081	0	0
MYO4	P32492	0	0.31	NIP1	P32497	0	0
MYO5	Q04439	0	0	NIP100	P33420	0	0
NAB3	P38996	0	0	NIP7	Q08962	0	0
NAB6	Q03735	0	0.39	NKP1	Q12493	0	0
NAM7	P30771	0	0.31	NMA1	Q06178	0	0
NAM8	Q00539	0	0	NMA111	P53920	0	0
NAM9	P27929	0	0	NMD3	P38861	0	0
NAN1	Q02931	0	0.01	NMD5	P46970	0.41	0
NAP1	P25293	0	0	NMT1	P14743	0	0
NAS6	P50086	0.18	0	NNF2	P53253	0	0
NAT1	P12945	0	0	NNK1	P36003	0	0
NAT4	Q04751	0	0	NOB1	Q08444	0	0
NAT5	Q08689	0	0	NOC2	P39744	0	0
NBA1	Q08229	0	0	NOC3	Q07896	0	0
NBL1	Q3E7Y6	0	0	NOG1	Q02892	0	0.02
NBP1	P52919	0	0	NOG2	P53742	0.03	0
NBP2	Q12163	0	0	NOP1	P15646	0.41	0.28
NBP35	P52920	0	0.31	NOP12	Q08208	0	0
NCA2	Q12374	0.41	0.54	NOP13	P53883	0	0
NCB2	Q92317	0	0	NOP14	Q99207	0	0
NCE102	Q12207	0	0	NOP15	P53927	0	0
NCL1	P38205	0	0	NOP19	P53317	0	0
NCP1	P16603	0	0.31	NOP2	P40991	0	0
NCR1	Q12200	0	0	NOP4	P37838	0	0.24
NDC1	P32500	0	0	NOP53	Q12080	0	0
NDE1	P40215	0	0	NOP56	Q12460	0	0
NDI1	P32340	0.58	0	NOP58	Q12499	0	0
NDJ1	Q12366	0	0	NOP7	P53261	0.12	0.1
NEO1	P40527	0.23	0.24	NOP8	Q08287	0	0
NET1	P47035	0.24	0.34	NOP9	P47077	0	0
NEW1	Q08972	0	0.01	NOT3	P06102	0	0.03
NFS1	P25374	0	0	NOT5	Q12514	0	0
NFT1	P0CE68	0	0	NPA3	P47122	0.01	0.3
NFU1	P32860	0	0	NPL3	Q01560	0	0
NGG1	P32494	0	0	NPL4	P33755	0	0
NGL3	Q03210	0	0	NPL6	P32832	0	0
NGR1	P32831	0	0	NPP1	P25353	0	0
NHA1	Q99271	0	0	NPR1	P22211	0	0.31

NPR2	P39923	0	0	OAF3	P36023	0	0
NPR3	P38742	0	0	OCA1	P50946	0	0
NPT1	P39683	0.17	0	OCA6	Q12454	0	0
NRD1	P53617	0.25	0	OCH1	P31755	0	0
NRG1	Q03125	0	0	OCT1	P35999	0	0
NRK1	P53915	0	0	ODC2	Q99297	0	0
NRP1	P32770	0	0	OGG1	P53397	0	0
NSA1	P53136	0	0	OKP1	P53298	0	0
NSA2	P40078	0	0	OLA1	P38219	0	0
NSE3	Q05541	0	0	OLE1	P21147	0	0.67
NSE4	P43124	0	0	OPI10	Q08202	0	0
NSE5	Q03718	0	0	OPT2	Q06593	0	0
NSL1	Q12143	0	0	OPY1	P38271	0	0
NSP1	P14907	0	0	OPY2	Q06810	0	0
NSR1	P27476	0	0	ORC5	P50874	0	0
NST1	P53935	0	0.31	ORC6	P38826	0.4	0
NTA1	P40354	0	0	ORM1	P53224	0	0.31
NTE1	Q04958	0	0	OSH2	Q12451	0.48	0.31
NTF2	P33331	0	0	OSH3	P38713	0	0
NTG1	P31378	0.12	0	OSH6	Q02201	0	0
NTH1	P32356	0	0.35	OSH7	P38755	0	0
NUC1	P08466	0	0	OSM1	P21375	0.41	0.24
NUG1	P40010	0.01	0.01	OST1	P41543	0	0.33
NUM1	Q00402	0.19	0.58	OST2	P46964	0	0
NUP100	Q02629	0	0	OST3	P48439	0.04	0.1
NUP120	P35729	0.21	0	OTU1	P43558	0.4	0
NUP133	P36161	0	0	OTU2	P38747	0	0
NUP145	P49687	0	0	OXP1	P28273	0	0.31
NUP157	P40064	0.25	0.33	OXR1	Q08952	0	0
NUP159	P40477	0.08	0	OYE2	Q03558	0.25	0.12
NUP170	P38181	0	0.02	OYE3	P41816	0	0
NUP188	P52593	0	0.31	P03871	P03871	0.25	0
NUP192	P47054	0	0.31	P03872	P03872	0	0
NUP2	P32499	0	0	P04936	P04936	0	0
NUP49	Q02199	0	0	P0CS90	P0CS90	0	0
NUP57	P48837	0	0	P0CT04	P0CT04	0	0
NUP60	P39705	0	0	P40587	P40587	0	0.54
NUP82	P40368	0	0	PAA1	Q12447	0.06	0.19
NUP84	P52891	0	0.24	PAB1	P04147	0	0
NUS1	Q12063	0	0	PAC1	P39946	0.41	0
NUT1	P53114	0	0	PAC10	P48363	0	0
NYV1	Q12255	0.23	0	PAC2	P39937	0.18	0
OAC1	P32332	0	0	PAF1	P38351	0	0

PAH1	P32567	0	0	PES4	P39684	0	0
PAM1	P37304	0	0	PET10	P36139	0.25	0
PAM16	P42949	0	0	PET111	P08468	0	0
PAM17	P36147	0	0	PET123	P17558	0	0
PAN1	P32521	0	0	PET54	P10834	0	0
PAN2	P53010	0	0	PET9	P18239	0	0.26
PAN5	P38787	0	0	PEX1	P24004	0	0
PAP1	P29468	0	0.33	PEX11	Q12462	0	0
PAR32	Q12515	0.09	0	PEX12	Q04370	0	0.33
PAT1	P25644	0	0.18	PEX13	P80667	0	0
PBA1	Q05778	0	0	PEX19	Q07418	0	0
PBP1	P53297	0.02	0	PEX25	Q02969	0	0
PBP2	P38151	0.48	0	PEX29	Q03370	0	0
PBP4	Q07362	0	0	PEX30	Q06169	0	0
PBY1	P38254	0	0	PEX6	P33760	0	0
PCD1	Q12524	0	0	PEX7	P39108	0	0
PCH2	P38126	0	0	PFD1	P46988	0.18	0
PCL9	Q12477	0	0	PFK1	P16861	0.22	0.33
PCM1	P38628	0.18	0.31	PFK2	P16862	0.04	0
PCS60	P38137	0	0	PFK26	P40433	0	0
PDA1	P16387	0	0.31	PFK27	Q12471	0	0
PDB1	P32473	0	0.26	PFY1	P07274	0	0
PDC1	P06169	0	0	PGA3	Q12746	0.23	0.08
PDC2	P32896	0	0.18	PGC1	Q08959	0	0.33
PDC5	P16467	0	0.44	PGD1	P40356	0	0
PDC6	P26263	0	0	PGI1	P12709	0	0
PDE1	P22434	0	0	PGK1	P00560	0.25	0.32
PDE2	P06776	0	0	PGM1	P33401	0.65	0.65
PDI1	P17967	0	0	PGM2	P37012	0	0
PDR11	P40550	0	0	PGS1	P25578	0	0
PDR12	Q02785	0	0	PHB1	P40961	0	0.02
PDR16	P53860	0.04	0	PHB2	P50085	0.25	0.66
PDR17	P53844	0	0	PHO4	P07270	0	0
PDR5	P33302	0	0	PHO8	P11491	0	0.33
PDS5	Q04264	0	0	PHO81	P17442	0	0.33
PDX1	P16451	0.05	0.46	PHO84	P25297	0.39	0.33
PDX3	P38075	0	0	PHO86	P46956	0.23	0.66
PEA2	P40091	0	0	PHO88	P38264	0	0.1
PEP1	P32319	0	0	PHO90	P39535	0	0.31
PEP12	P32854	0	0	PHO91	P27514	0	0.08
PEP4	P07267	0	0.15	PHR1	P05066	0	0
PEP5	P12868	0	0	PIB2	P53191	0	0
PER33	Q12144	0.41	0	PIF1	P07271	0	0

PIK1	P39104	0	0	PRD1	P25375	0.23	0
PIL1	P53252	0	0	PRE10	P21242	0.23	0.54
PIM1	P36775	0	0.01	PRE2	P30656	0	0
PIN4	P34217	0	0	PRE3	P38624	0	0
PIS1	P06197	0.17	0.15	PRE4	P30657	0	0
PKC1	P24583	0	0.33	PRE5	P40302	0	0.07
PLB1	P39105	0	0	PRE6	P40303	0	0.27
PLC1	P32383	0	0	PRE7	P23724	0.41	0.33
PLP2	Q12017	0	0	PRE8	P23639	0	0
PMA1	P05030	0	0	PRE9	P23638	0	0
PMC1	P38929	0	0	PRI1	P10363	0.18	0.35
PMD1	P32634	0	0	PRM8	P53174	0	0
PMI40	P29952	0	0.15	PRO1	P32264	0	0
PMR1	P13586	0	0.28	PRO2	P54885	0.36	0
PMT1	P33775	0.04	0.55	PRO3	P32263	0	0.33
PMT2	P31382	0.34	0.47	PRP16	P15938	0	0
PMT3	P47190	0	0	PRP19	P32523	0	0
PMT4	P46971	0.18	0.26	PRP28	P23394	0.18	0
PMT5	P52867	0	0	PRP39	P39682	0	0
PMU1	P36069	0	0.44	PRP43	P53131	0.01	0.23
PNC1	P53184	0	0.64	PRP46	Q12417	0	0
PNO1	Q99216	0	0	PRP5	P21372	0	0
POB3	Q04636	0.09	0.04	PRP8	P33334	0.23	0
POC4	Q12245	0	0	PRS1	P32895	0	0
POL1	P13382	0	0	PRS2	P38620	0	0
POL12	P38121	0	0	PRS3	P38689	0.17	0
POL2	P21951	0	0	PRS4	P38063	0.16	0
POL3	P15436	0.41	0	PRS5	Q12265	0	0
POL31	P46957	0	0	PRT1	P06103	0	0
POL5	P39985	0	0.33	PRX1	P34227	0	0
POM152	P39685	0	0	PSA1	P41940	0	0
POM33	Q12164	0	0	PSD1	P39006	0	0
POR1	P04840	0	0.33	PSE1	P32337	0.43	0.57
POX1	P13711	0	0	PSF1	Q12488	0	0.31
PPE1	P38796	0	0	PSH1	Q12161	0	0
PPM1	Q04081	0	0	PSK1	P31374	0	0.24
PPM2	Q08282	0	0	PSK2	Q08217	0	0
PPN1	Q04119	0.25	0.33	PSP2	P50109	0	0
PPS1	P38148	0	0	PSR1	Q07800	0	0
PPT1	P53043	0.15	0	PST2	Q12335	0	0.33
PPZ2	P33329	0.42	0	PSY2	P40164	0	0
PRB1	P09232	0	0	PSY4	P38193	0	0
PRC1	P00729	0	0	PTA1	Q01329	0	0

PTC2	P39966	0	0	RAD9	P14737	0	0
PTC3	P34221	0	0	RAM1	P22007	0	0
PTC4	P38089	0	0	RAP1	P11938	0	0
PTC5	Q12511	0	0	RAS1	P01119	0	0
PTI1	P39927	0	0	RAS2	P01120	0	0
PTM1	P32857	0.25	0.44	RAV1	P47104	0	0
PTR2	P32901	0	0.06	RAX2	Q12465	0	0
PTR3	P43606	0	0	RBA50	Q04418	0.5	0
PUB1	P32588	0	0	RBG1	P39729	0	0
PUF2	Q12221	0	0	RBG2	P53295	0.3	0.07
PUF3	Q07807	0	0.07	RBL2	P48606	0	0
PUF4	P25339	0.65	0.56	RCK2	P38623	0	0
PUF6	Q04373	0.17	0.15	RCL1	Q08096	0	0
PUP1	P25043	0	0	RCN2	Q12044	0	0
PUP2	P32379	0	0	RCO1	Q04779	0	0
PUP3	P25451	0	0	RDH54	P38086	0	0
PUS1	Q12211	0.23	0.66	RDI1	Q12434	0	0
PUS2	P53167	0	0	RDL1	Q12305	0	0
PUT4	P15380	0	0	RDS3	Q06835	0	0
PWP1	P21304	0	0	REB1	P21538	0	0
PWP2	P25635	0	0	REG1	Q00816	0	0.18
PXR1	P53335	0	0	REG2	P38232	0	0
PYC1	P11154	0.5	0.89	REH1	Q06709	0	0
PYC2	P32327	0	0.32	REI1	P38344	0	0
PYK2	P52489	0.23	0	RER2	P35196	0	0
PZF1	P39933	0	0	RET1	P22276	0.67	0.33
Q0255	P03881	0	0	RET2	P43621	0	0.65
QCR2	P07257	0	0.46	RET3	P53600	0.02	0.33
QCR7	P00128	0	0.33	REV3	P14284	0	0
QDR2	P40474	0	0.33	REX2	P54964	0.18	0
QNS1	P38795	0.18	0	REX3	Q12090	0	0
QRI1	P43123	0	0.33	REX4	Q08237	0	0
RAD1	P06777	0	0	RFA1	P22336	0	0
RAD17	P48581	0	0	RFA2	P26754	0.02	0
RAD23	P32628	0	0	RFA3	P26755	0	0
RAD24	P32641	0	0	RFC1	P38630	0.25	0.33
RAD26	P40352	0	0	RFC2	P40348	0.22	0.09
RAD3	P06839	0.18	0	RFC3	P38629	0.5	0.55
RAD5	P32849	0	0	RFS1	P38234	0	0.33
RAD50	P12753	0	0	RGA2	Q06407	0.23	0
RAD51	P25454	0	0	RGD2	P43556	0	0
RAD52	P06778	0	0	RGI1	P40043	0	0
RAD54	P32863	0	0	RGP1	P16664	0	0

RGR1	P19263	0.4	0.63	ROD1	Q02805	0	0
RHO1	P06780	0	0	ROG1	P53118	0	0
RHO2	P06781	0	0	ROK1	P45818	0	0
RHO3	Q00245	0	0.33	ROM1	P53046	0.48	0
RHO5	P53879	0	0.23	ROM2	P51862	0.23	0
RHR2	P41277	0	0.25	ROT2	P38138	0.01	0
RIA1	P53893	0.26	0	ROX1	P25042	0	0
RIB1	P38066	0	0	ROY1	Q04847	0	0
RIB2	Q12362	0	0	RPA12	P32529	0	0
RIB3	Q99258	0.41	0.61	RPA135	P22138	0.65	0.06
RIB4	P50861	0	0.98	RPA190	P10964	0.33	0.19
RIC1	P40395	0	0	RPA34	P47006	0	0
RIF1	P29539	0	0	RPA43	P46669	0	0
RIM1	P32445	0	0	RPA49	Q01080	0	0
RIM13	Q03792	0	0	RPB10	P22139	1	1
RIM15	P43565	0	0	RPB11	P38902	1	1
RIM4	P38741	0	0	RPB2	P08518	1	1
RIO1	Q12196	0	0.33	RPB3	P16370	1	1
RIO2	P40160	0.29	0.34	RPB4	P20433	1	1
RIX1	P38883	0.25	0	RPB5	P20434	1	1
RIX7	Q07844	0	0	RPB7	P34087	1	1
RKM1	Q08961	0	0	RPB8	P20436	1	1
RKM5	Q12367	0	0	RPB9	P27999	1	0
RKR1	Q04781	0.21	0.31	RPC10	P40422	0.95	0.91
RLF2	Q12495	0	0	RPC19	P28000	0.06	0
RLI1	Q03195	0	0.32	RPC31	P17890	0	0
RLP24	Q07915	0	0	RPC34	P32910	0	0
RLP7	P40693	0	0.31	RPC37	P36121	0	0
RMD1	Q03441	0	0	RPC40	P07703	0.01	0
RMD8	P43620	0	0	RPC53	P25441	0	0
RMT2	Q03305	0	0	RPC82	P32349	0	0
RNA1	P11745	0.49	0.71	RPD3	P32561	0.06	0
RNA14	P25298	0	0	RPE1	P46969	0.64	0.57
RNA15	P25299	0	0	RPF1	P38805	0	0
RNH202	Q05635	0	0	RPF2	P36160	0	0
RNH203	Q12338	0	0	RPG1	P38249	0	0.02
RNQ1	P25367	0	0	RPL10	P41805	0	0
RNR1	P21524	0	0	RPL11A	P0C0W9	0.5	0
RNR2	P09938	0	0	RPL12A;RPL12B	P0CX53	0	0
RNR3	P21672	0	0	RPL13A	Q12690	0	0
RNR4	P49723	0	0	RPL13B	P40212	0	0.06
RNT1	Q02555	0	0	RPL14A	P36105	0	0
RNY1	Q02933	0	0	RPL14B	P38754	0	0

RPL15A	P05748	0	0	RPL6B	P05739	0	0
RPL15B	P54780	0	0	RPL7A	P05737	0	0
RPL16A	P26784	0	0	RPL7B	Q12213	0	0
RPL16B	P26785	0	0	RPL8A	P17076	0	0
RPL17A	P05740	0	0	RPL8B	P29453	0	0
RPL17B	P46990	0	0	RPL9A	P05738	0	0
RPL18A;RPL18B	P0CX49	0	0	RPL9B	P51401	0	0
RPL19A;RPL19B	P0CX82	0	0	RPM2	Q02773	0	0.33
RPL1A;RPL1B	P0CX43	0	0	RPN1	P38764	0	0
RPL20A;RPL20B	P0CX23	0	0	RPN10	P38886	0	0
RPL21A	Q02753	0	0	RPN11	P43588	0	0
RPL21B	Q12672	0.75	0.33	RPN12	P32496	0	0
RPL22A	P05749	0	0.1	RPN13	O13563	0	0
RPL23A;RPL23B	P0CX41	0	0	RPN14	P53196	0	0
RPL24A	P04449	0	0	RPN2	P32565	0	0.02
RPL24B	P24000	0	0	RPN3	P40016	0	0
RPL25	P04456	0	0	RPN5	Q12250	0	0
RPL26A	P05743	0	0	RPN6	Q12377	0.13	0.05
RPL26B	P53221	0	0	RPN7	Q06103	0	0
RPL27A	P0C2H6	0	0.01	RPN8	Q08723	0	0.09
RPL28	P02406	0	0.1	RPN9	Q04062	0.01	0.05
RPL29	P05747	0.7	0.29	RPO21	P04050	1	1
RPL2A;RPL2B	P0CX45	0	0.32	RPO26	P20435	1	1
RPL3	P14126	0	0.33	RPO31	P04051	0.08	0
RPL30	P14120	0	0	RPO41	P13433	0.23	0
RPL31A	P0C2H8	0	0.27	RPP0	P05317	0	0
RPL31B	P0C2H9	0	0	RPP1	P38786	0	0
RPL32	P38061	0	0	RPP1A	P05318	0.02	0
RPL33A	P05744	0	0.32	RPP1B	P10622	0	0
RPL33B	P41056	0	0.33	RPP2A	P05319	0	0
RPL34B	P40525	0	0	RPP2B	P02400	0	0
RPL35A;RPL35B	P0CX84	0	0	RPS0A	P32905	0	0.06
RPL36A	P05745	0	0	RPS10A	Q08745	0	0.33
RPL36B	O14455	0	0	RPS10B	P46784	0	0
RPL37A	P49166	0	0.65	RPS11A;RPS11B	P0CX47	0	0.16
RPL37B	P51402	0.18	0.33	RPS12	P48589	0	0
RPL38	P49167	0	0	RPS13	P05756	0	0
RPL42A;RPL42B	P0CX28	0.24	0.67	RPS14A	P06367	0	0
RPL43A;RPL43B	P0CX25	0	0	RPS15	Q01855	0	0
RPL4A	P10664	0	0	RPS16A;RPS16B	P0CX52	0	0
RPL4B	P49626	0	0	RPS17A	P02407	0	0
RPL5	P26321	0	0.33	RPS18A;RPS18B	P0CX55	0	0
RPL6A	Q02326	0	0	RPS19A	P07280	0	0

RPS1A	P33442	0	0	RRP6	Q12149	0	0
RPS1B	P23248	0	0	RRP8	P38961	0	0.31
RPS2	P25443	0	0.02	RRP9	Q06506	0	0
RPS20	P38701	0	0.33	RRT14	P40470	0	0
RPS21A	P0C0V8	0	0.28	RSA3	Q05942	0	0
RPS21B	Q3E754	0	0	RSA4	P25382	0	0
RPS22A	P0C0W1	0.18	0.33	RSC1	P53236	0	0
RPS23A;RPS23B	P0CX29	0	0	RSC2	Q06488	0	0.31
RPS24A;RPS24B	P0CX31	0	0	RSC3	Q06639	0	0
RPS25B	P0C0T4	0	0	RSC30;YHR054C	P38780	0	0
RPS26A	P39938	0.22	0	RSC4	Q02206	0	0.24
RPS27A	P35997	0	0	RSC58	Q07979	0	0
RPS28B	P0C0X0	0	0	RSC6	P25632	0	0
RPS29A	P41057	0	0.09	RSC8	P43609	0	0.1
RPS29B	P41058	0	0.33	RSC9	Q03124	0	0
RPS3	P05750	0	0	RSE1	Q04693	0	0
RPS30A;RPS30B	P0CX33	0	0	RSF2	P46974	0	0
RPS31	P05759	0	0	RSM10	Q03201	0	0.33
RPS4A;RPS4B	P0CX35	0	0.33	RSM19	P53733	0	0
RPS5	P26783	0	0	RSM23	Q01163	0	0
RPS6A;RPS6B	P0CX37	0	0	RSM24	Q03976	0	0
RPS7A	P26786	0	0	RSM25	P40496	0	0
RPS7B	P48164	0	0	RSM27	P53305	0	0
RPS8A;RPS8B	P0CX39	0	0	RSM28	Q03430	0	0
RPS9A	O13516	0	0	RSM7	P47150	0	0
RPS9B	P05755	0	0.01	RSN1	Q03516	0	0
RPT1	P33299	0	0.33	RSP5	P39940	0	0
RPT2	P40327	0	0.45	RSR1	P13856	0	0
RPT3	P33298	0.12	0.34	RTC5	Q12108	0	0
RPT4	P53549	0.24	0.64	RTF1	P53064	0	0.01
RPT5	P33297	0	0	RTG1	P32607	0	0
RPT6	Q01939	0	0.33	RTG2	P32608	0	0.44
RRB1	Q04225	0	0	RTN1	Q04947	0	0
RRG9	P40156	0	0	RTN2	Q12443	0	0.33
RRP1	P35178	0	0.01	RTR1	P40084	0.73	1
RRP12	Q12754	0.29	0	RTS1	P38903	0.47	0
RRP14	P36080	0	0	RTS3	P53289	0	0
RRP15	Q06511	0	0	RTT10	Q08924	0	0
RRP17	Q04031	0	0	RTT101	P47050	0	0
RRP3	P38712	0.23	0	RTT103	Q05543	0	0
RRP43	P25359	0	0	RTT107	P38850	0	0
RRP46	P53256	0.25	0	RUD3	Q12234	0.25	0
RRP5	Q05022	0.22	0.25	RVB1	Q03940	0.23	0

RVB2	Q12464	0	0	SEC10	Q06245	0	0
RVS161	P25343	0.21	0.33	SEC11	P15367	0	0
RVS167	P39743	0.34	0.57	SEC12	P11655	0	0
RXT2	P38255	0.12	0	SEC13	Q04491	0	0
RXT3	Q07458	0	0	SEC14	P24280	0	0
SAC1	P32368	0.09	0.54	SEC15	P22224	0	0
SAC6	P32599	0	0	SEC16	P48415	0	0.33
SAH1	P39954	0.06	0.1	SEC17	P32602	0	0
SAK1	P38990	0	0	SEC18	P18759	0.01	0.31
SAM1	P10659	0	0	SEC21	P32074	0.01	0.33
SAM2	P19358	0	0	SEC22	P22214	0	0
SAM3	Q08986	0	0	SEC23	P15303	0	0
SAN1	P22470	0.01	0	SEC24	P40482	0	0
SAP155	P43612	0	0	SEC26	P41810	0.17	0.18
SAP185	P40856	0	0	SEC27	P41811	0	0
SAR1	P20606	0.2	0.32	SEC28	P40509	0.39	0
SAS10	Q12136	0	0	SEC3	P33332	0	0
SBA1	P28707	0.01	0	SEC31	P38968	0	0
SBE2	P42223	0	0	SEC39	Q12745	0	0
SBH2	P52871	0	0	SEC4	P07560	0	0
SBP1	P10080	0	0	SEC53	P07283	0.37	0.45
SCD6	P45978	0	0	SEC6	P32844	0	0
SCH9	P11792	0	0	SEC61	P32915	0.42	0.89
SCJ1	P25303	0.15	0.04	SEC62	P21825	0.23	0.33
SCL1	P21243	0	0	SEC63	P14906	0	0
SCO1	P23833	0	0	SEC65	P29478	0	0.2
SCO2	P38072	0	0	SEC7	P11075	0	0.21
SCP1	Q08873	0	0	SEC72	P39742	0	0.35
SCP160	P06105	0	0	SEC9	P40357	0	0
SCS2	P40075	0.02	0.07	SED4	P25365	0	0
SCS7	Q03529	0	0.28	SED5	Q01590	0	0
SCW4	P53334	0	0	SEF1	P34228	0	0
SCY1	P53009	0.25	0	SEH1	P53011	0.23	0
SDA1	P53313	0	0	SEN1	Q00416	0.67	0.89
SDH1	Q00711	0	0	SER1	P33330	0.25	0.9
SDH2	P21801	0	0	SER3	P40054	0.67	0.66
SDH3	P33421	0	0	SER33	P40510	0	0.03
SDO1	Q07953	0	0	SES1	P07284	0	0.33
SDS23	P53172	0.25	0	SET4	P42948	0	0
SDS24	P38314	0.4	0.66	SET5	P38890	0	0
SDS3	P40505	0	0	SEY1	Q99287	0	0
SEA4	P38164	0	0	SFB2	P53953	0	0.08
SEC1	P30619	0	0	SFB3	P38810	0	0

SFH1	Q06168	0	0	SLA2	P33338	0	0
SFH5	P47008	0	0.07	SLC1	P33333	0	0.66
SFI1	Q12369	0	0	SLD3	P53135	0	0
SFT2	P38166	0	0	SLF1	Q12034	0	0
SGD1	Q06132	0	0.31	SLG1	P54867	0	0
SGF29	P25554	0	0	SLK19	Q08581	0	0
SGM1	P47166	0	0	SLM4	P38247	0	0
SGN1	P40561	0	0	SLM5	P25345	0	0
SGO1	Q08490	0	0	SLT2	Q00772	0	0.33
SGT1	Q08446	0	0	SLU7	Q02775	0	0
SGT2	Q12118	0	0	SLX9	P53251	0	0
SHE1	P38200	0	0.33	SLY1	P22213	0.09	0.27
SHE10	P53075	0	0.27	SMA1	Q02651	0	0
SHE2	P36068	0	0.33	SMC1	P32908	0	0
SHE3	P38272	0	0	SMC2	P38989	0	0
SHM1	P37292	0	0	SMC3	P47037	0	0
SHM2	P37291	0.24	0.31	SMC4	Q12267	0.23	0
SHO1	P40073	0.18	0	SMC5	Q08204	0	0
SHP1	P34223	0	0	SMC6	Q12749	0	0
SHR3	Q02774	0.18	0	SMF1	P38925	0	0
SHS1	Q07657	0	0	SMF3	Q12078	0	0
SIL1	Q08199	0	0	SMI1	P32566	0	0
SIN3	P22579	0.3	0.05	SMK1	P41808	0	0
SIN4	P32259	0	0	SMT3	Q12306	0.18	0
SIP3	P38717	0	0.33	SMY1	P32364	0	0
SIP4	P46954	0	0	SMY2	P32909	0	0
SIR1	P21691	0	0	SNA2	P56508	0	0
SIR4	P11978	0	0	SNA3	P14359	0	0.33
SIS1	P25294	0	0	SNC1	P31109	0	0
SIS2	P36024	0.23	0.24	SNC2	P33328	0	0
SIT1	P39980	0.23	0	SNF1	P06782	0	0
SIT4	P20604	0	0	SNF12	P53628	0	0
SIZ1	Q04195	0	0	SNF2	P22082	0.18	0
SKG1	P36169	0	0	SNF3	P10870	0	0
SKI2	P35207	0	0	SNF4	P12904	0	0.54
SKI3	P17883	0.23	0.31	SNF5	P18480	0	0
SKI7	Q08491	0	0	SNF7	P39929	0	0
SKI8	Q02793	0	0	SNG1	P46950	0	0
SKN1	P33336	0	0	SNL1	P40548	0	0.15
SKP1	P52286	0	0	SNQ2	P32568	0	0
SKP2	P42843	0	0	SNT2	P53127	0	0
SKY1	Q03656	0	0	SNU114	P36048	0.23	0
SLA1	P32790	0	0.88	SNU13	P39990	0.01	0

SNU23	Q12368	0	0	SRM1	P21827	0	0
SNX3	Q08826	0.23	0	SRO9	P25567	0	0
SNX4	P47057	0	0	SRP1	Q02821	0.05	0.09
SNX41	Q04053	0	0	SRP101	P32916	0	0
SOD1	P00445	0	0	SRP102	P36057	0	0
SOG2	Q08817	0	0	SRP14	P38985	0	0
SOL2	P37262	0	0	SRP40	P32583	0	0
SOR1	P35497	0	0	SRP54	P20424	0	0
SOV1	Q04748	0	0	SRP68	P38687	0	0
sp	sp	0	0	SRP72	P38688	0	0
SPA2	P23201	0	0	SRS2	P12954	0	0
SPB4	P25808	0.23	0	SRV2	P17555	0	0
SPC105	P53148	0	0	SRY1	P36007	0	0
SPC19	Q03954	0	0	SSA1	P10591	0	0
SPC2	Q04969	0	0	SSA2	P10592	0	0
SPC3	Q12133	0	0	SSA3	P09435	0	0
SPC42	P36094	0	0	SSA4	P22202	0	0
SPE3	Q12074	0.18	0	SSB1	P11484	0	0
SPE4	Q12455	0	0	SSB2	P40150	0	0
SPF1	P39986	0	0	SSD1	P24276	0.08	0.57
SPH1	Q06160	0	0	SSE1	P32589	0	0
SPN1	Q06505	0	0	SSE2	P32590	0.25	0.33
SPO13	P23624	0	0	SSF1	P38789	0.25	0
SPO14	P36126	0	0	SSF2	Q12153	0	0
SPO20	Q04359	0	0	SSH1	P38353	0.24	0.25
SPO71	Q03868	0	0.65	SSK2	P53599	0	0
SPP41	P38904	0	0	SSK22	P25390	0	0
SPR3	P41901	0	0	SSM4	P40318	0	0
SPS1	P08458	0	0	SSN2	P38931	0	0
SPS2	P08459	0	0	SSN3	P39073	0	0
SPT15	P13393	0	0	SSO1	P32867	0.17	0.11
SPT16	P32558	0	0.02	SSO2	P39926	0	0
SPT23	P35210	0	0	SSP120	P39931	0.01	0
SPT4	P32914	0.48	0.33	SSQ1	Q05931	0	0
SPT5	P27692	0.07	0	SSS1	P35179	0	0
SPT6	P23615	0.03	0.29	SST2	P11972	0	0
SPT7	P35177	0	0	SSY5	P47002	0	0
SPT8	P38915	0	0	SSZ1	P38788	0	0.33
SQT1	P35184	0	0	STB1	P42845	0	0
SRB2	P34162	0	0	STB5	P38699	0	0
SRB6	P32570	0	0	STE11	P23561	0	0
SRB7	P47822	0	0	STE13	P33894	0	0.15
SRB8	P25648	0.23	0.31	STE18	P18852	0	0

STE2	D6VTK4	0	0	SYP1	P25623	0.05	0
STE20	Q03497	0	0	SYS1	P41544	0	0.33
STE23	Q06010	0	0	SYT1	Q06836	0	0
STE24	P47154	0.1	0.33	TAD2	P47058	0	0.33
STE4	P18851	0	0	TAE1	P38340	0	0
STE6	P12866	0	0.33	TAE2	Q12532	0	0.55
STH1	P32597	0	0	TAF1	P46677	0	0
STI1	P15705	0	0	TAF10	Q12030	0	0
STM1	P39015	0.21	0.33	TAF11	Q04226	0	0
STO1	P34160	0	0	TAF12	Q03761	0	0
STT3	P39007	0.07	0	TAF13	P11747	0.23	0
STT4	P37297	0.23	0.3	TAF14	P35189	0	0
STU2	P46675	0	0	TAF5	P38129	0	0
STV1	P37296	0.06	0	TAF6	P53040	0	0
SUA7	P29055	0	0	TAF8	Q03750	0	0.24
SUB1	P54000	0	0	TAH11	P47112	0.23	0
SUB2	Q07478	0	0.33	TAH18	Q12181	0.23	0
SUI1	P32911	0	0	TAL1	P15019	0	0
SUI2	P20459	0	0	TAN1	P53072	0	0
SUI3	P09064	0	0	TAO3	P40468	0	0.55
SUL1	P38359	0	0	TAP42	Q04372	0.22	0.29
SUM1	P46676	0	0	TAT1	P38085	0.03	0
SUN4	P53616	0	0	TBF1	Q02457	0.23	0
SUP35	P05453	0	0.04	TBS1	P38114	0	0
SUP45	P12385	0	0	TCB1	Q12466	0.01	0.37
SUR2	P38992	0	0.56	TCB2	P48231	0	0
SUR4	P40319	0	0	TCB3	Q03640	0	0
SVF1	Q05515	0	0	TCP1	P12612	0	0
SVL3	Q03088	0	0	TDA10	P42938	0	0
SWA2	Q06677	0.18	0	TDA11	P38854	0	0
SWC3	P31376	0	0	TDA2	P40045	0	0
SWC7	Q06707	0	0	TDA3	P38758	0	0
SWD1	P39706	0	0	TDH1	P00360	0	0.33
SWE1	P32944	0	0	TDH2	P00358	0	0.33
SWH1	P35845	0	0.24	TDH3	P00359	0	0.33
SWI3	P32591	0	0	TEC1	P18412	0	0
SWI6	P09959	0	0	TEF1;TEF2	P02994	0	0
SWP1	Q02795	0	0	TEF4	P36008	0.22	0
SWP82	P43554	0.25	0	TEL1	P38110	0	0
SXM1	Q04175	0.13	0.36	TEL2	P53038	0.23	0
SYG1	P40528	0	0	TEM1	P38987	0	0
SYH1	Q02875	0	0	TEP1	P53916	0	0
SYN8	P31377	0	0	TEX1	P53851	0	0

TFA1	P36100	0	0	TIR1	P10863	0	0
TFA2	P36145	0	0	TKL1	P23254	0.44	0.04
TFB1	P32776	0	0	TLG1	Q03322	0.23	0
TFB2	Q02939	0	0.76	TLG2	Q08144	0	0
TFB3	Q03290	0	0	TMA108	P40462	0.5	0.57
TFC4	P33339	0	0	TMA16	Q08687	0	0.23
TFC6	Q06339	0.23	0	TMA19	P35691	0	0
TFG1	P41895	0	0	TMA20	P89886	0	0
TFG2	P41896	0	0	TMA22	P47089	0	0
TGL1	P34163	0.25	0.66	TMA23	Q03525	0	0
TGL4	P36165	0	0.87	TMA46	Q12000	0	0
TGL5	Q12043	0	0	TMN3	P40071	0	0
THG1	P53215	0	0	TNA1	P53322	0	0.31
THI20	Q08224	0	0.67	TOA2	P32774	0	0
THI21	Q08975	0	0.31	TOF1	P53840	0.41	0
THI3	Q07471	0	0.33	TOM1	Q03280	0	0.3
THI7	Q05998	0	0	TOM20	P35180	0	0
THI80	P35202	0.4	0	TOM22	P49334	0	0
THO1	P40040	0	0	TOM40	P23644	0.05	0
THO2	P53552	0	0	TOM5	P80967	0	0
THP1	Q08231	0	0	TOM70	P07213	0.01	0.3
THP2	O13539	0	0	TOM71	P38825	0.26	0
THR1	P17423	0.58	0	TOP1	P04786	0	0
THR4	P16120	0.01	0	TOP2	P06786	0	0.23
THS1	P04801	0	0	TOR1	P35169	0	0
TIF1;TIF2	P10081	0	0	TOR2	P32600	0	0.33
TIF11	P38912	0	0	TPC1	P53257	0	0
TIF3	P34167	0	0	TPD3	P31383	0.01	0
TIF34	P40217	0	0	TPI1	P00942	0	0
TIF35	Q04067	0	0	TPK1	P06244	0	0
TIF4631	P39935	0	0	TPK2	P06245	0	0
TIF4632	P39936	0.23	0	TPM1	P17536	0	0
TIF5	P38431	0	0	TPM2	P40414	0	0
TIF6	Q12522	0	0	TPO3	Q06451	0	0
TIM10	P87108	0	0	TPO5	P36029	0	0
TIM11	P81449	0	0	TPS1	Q00764	0	0
TIM13	P53299	0	0	TPS2	P31688	0	0.33
TIM23	P32897	0	0	TPS3	P38426	0.06	0.33
TIM44	Q01852	0	0	TPT1	Q12272	0	0
TIM50	Q02776	0.01	0.22	TRA1	P38811	0.23	0
TIM54	P47045	0	0	TRE1	Q08919	0	0
TIM9	O74700	0	0	TRE2	Q08693	0	0
TIP20	P33891	0	0	TRK1	P12685	0	0

TRL1	P09880	0.23	0	UBA2	P52488	0	0.3
TRM1	P15565	0	0	UBA3	Q99344	0	0
TRM12	Q04235	0	0	UBA4	P38820	0	0
TRM3	Q07527	0	0	UBC1	P21734	0.12	0.15
TRM44	Q02648	0	0	UBC13	P52490	0	0.31
TRM5	P38793	0	0.33	UBC6	P33296	0	0
TRM8	Q12009	0.14	0	UBC9	P50623	0	0.31
TRM82	Q03774	0	0	UBI4	P0CG63	0.25	0
TRM9	P49957	0	0	UBP1	P25037	0	0
TRP2	P00899	0	0	UBP10	P53874	0	0
TRP3	P00937	0.17	0.22	UBP11	P36026	0	0
TRP4	P07285	0	0	UBP14	P38237	0	0
TRP5	P00931	0	0	UBP15	P50101	0	0.86
TRR1	P29509	0	0	UBP2	Q01476	0	0
TRS120	Q04183	0	0	UBP3	Q01477	0.49	0.64
TRS130	Q03660	0	0.35	UBP6	P43593	0	0
TRS31	Q03337	0	0	UBP9	P39967	0	0
TRS33	Q99394	0	0	UBR1	P19812	0	0
TRS85	P46944	0	0	UBR2	Q07963	0	0
TRX1	P22217	0	0	UBX5	Q06682	0	0
TRX2	P22803	0	0	UBX7	P38349	0	0
TRX3	P25372	0	0	UFD1	P53044	0	0
TRZ1	P36159	0	0	UFD2	P54860	0	0.19
TSA1	P34760	0.22	0	UFD4	P33202	0.41	0.56
TSC10	P38342	0	0	UGA1	P17649	0	0.33
TSC13	Q99190	0	0.1	UGA3	P26370	0	0
TSL1	P38427	0	0.33	UGP1	P32861	0.18	0
TSR1	Q07381	0	0	UGX2	P32772	0	0
TSR2	Q06672	0	0	UIP3	P39547	0	0.23
TSR4	P25040	0.04	0	ULP1	Q02724	0	0
TUB1	P09733	0	0.02	ULP2	P40537	0	0
TUB2	P02557	0	0.32	ULS1	Q08562	0	0
TUB3	P09734	0	0	UME6	P39001	0	0.31
TUF1	P02992	0	0	UMP1	P38293	0	0
TUM1	Q08686	0	0	UPC2	Q12151	0	0
TUP1	P16649	0	0	URA1	P28272	0	0
TVP18	Q04767	0.25	0.33	URA2	P07259	0	0.33
TVP23	P38962	0	0	URA5	P13298	0	0
TWF1	P53250	0	0	URA6	P15700	0	0
TYR1	P20049	0.25	0.31	URA7	P28274	0	0
TYS1	P36421	0	0	URA8	P38627	0.25	0.33
TYW1	Q08960	0	0	URB1	P34241	0.01	0
UBA1	P22515	0.01	0.28	URB2	P47108	0	0

URK1	P27515	0	0	VPS1	P21576	0	0.01
USA1	Q03714	0	0	VPS13	Q07878	0.01	0.4
USO1	P25386	0.26	0.48	VPS16	Q03308	0	0
UTP10	P42945	0.47	0.38	VPS17	P32913	0	0
UTP13	Q05946	0	0	VPS20	Q04272	0	0
UTP14	Q04500	0	0	VPS21	P36017	0	0
UTP15	Q04305	0	0	VPS24	P36095	0	0
UTP18	P40362	0	0	VPS27	P40343	0	0
UTP20	P35194	0	0.35	VPS28	Q02767	0	0
UTP21	Q06078	0.23	0.33	VPS29	P38759	0	0
UTP22	P53254	0	0.3	VPS3	P23643	0	0
UTP25	P40498	0	0	VPS30	Q02948	0	0
UTP4	Q06679	0	0	VPS35	P34110	0	0
UTP6	Q02354	0	0	VPS45	P38932	0	0
UTP7	P40055	0	0	VPS51	P36116	0	0
UTP8	P53276	0	0.31	VPS54	Q12071	0	0
UTP9	P38882	0	0	VPS66	Q06508	0	0.33
UTR1	P21373	0	0	VPS68	Q12016	0	0
UTR2	P32623	0	0	VPS70	P47161	0	0
VAC8	P39968	0.36	0.6	VPS74	Q06385	0	0
VAM6	Q07468	0	0	VPS8	P39702	0	0
VAN1	P23642	0	0	VRG4	P40107	0	0
VAR1	P02381	0	0	VRP1	P37370	0	0
VAS1	P07806	0	0	VTC2	P43585	0.02	0.33
VBA4	Q04602	0	0	VTC3	Q02725	0.41	0.67
VFA1	P40080	0	0	VTC4	P47075	0.52	0.81
VHS1	Q03785	0	0	VTI1	Q04338	0	0.15
VHS3	Q08438	0	0	VTS1	Q08831	0	0
VID27	P40157	0	0	WBP1	P33767	0.04	0.12
VIP1	Q06685	0.22	0.17	WHI3	P34761	0.21	0.33
VMA1	P17255	0	0.23	WHI4	Q07655	0	0
VMA10	P48836	0	0	WRS1	Q12109	0	0.04
VMA11	P32842	0	0.31	WTM1	Q12363	0	0
VMA13	P41807	0	0.28	WWM1	P43582	0	0
VMA2	P16140	0	0	XRN1	P22147	0	0.31
VMA22	P38784	0	0	XRS2	P33301	0	0
VMA4	P22203	0	0	YAE1	P47118	0	0
VMA5	P31412	0	0.04	YAL037C-A	Q3E741	0	0
VMA6	P32366	0	0.07	YAL063C-A	Q3E791	0	0
VMA7	P39111	0	0	YAL064W	P39711	0	0
VMA8	P32610	0.52	0.6	YAL066W	P39710	0	0
VMA9	Q3E7B6	0	0	YAP1	P19880	0	0
VPH1	P32563	0	0.42	YAP1801	P38856	0	0

YAP3	P38749	0	0	YDR266C	Q05580	0	0
YAR028W	P39548	0	0.24	YDR306C	Q06640	0	0
YAR1	P46683	0	0	YDR307W	Q06644	0.4	0
YBL036C	P38197	0	0.31	YDR341C	Q05506	0	0
YBP1	P38315	0	0.24	YDR348C	Q05518	0	0
YBR056W	P38081	0	0	YDR352W	Q06328	0	0
YBR062C	P38239	0	0	YDR365W-B	P0C2I7	0	0
YBR064W	P38240	0	0	YDR366C	P87287	0	0
YBR074W	P38244	0	0	YDR370C	Q06349	0	0
YBR121C-A	P0C5L4	0	0	YDR444W	Q04093	0	0
YBR126W-A	Q8TGU7	0	0	YDR476C	Q03362	0	0
YBR197C	P38306	0	0	YDR543C	Q03051	0	0
YBT1	P32386	0.06	0.02	YEF3	P16521	0	0.04
YCF1	P39109	0	0.16	YEH1	Q07804	0	0.54
YCK1	P23291	0	0	YEL023C	P39992	0.23	0
YCK2	P23292	0	0	YEL043W	P32618	0	0
YCL012C	Q8J0M4	0	0	YEL047C	P32614	0.42	0.49
YCP4	P25349	0	0.06	YEL1	P34225	0	0.31
YCR015C	P25616	0	0	YER064C	P40041	0	0
YCR016W	P25617	0	0	YER077C	P40050	0	0
YCR045W-A	Q8TGQ2	0	0	YER079W	P40052	0	0
YCR051W	P25631	0	0	YER138W-A	P25561	0	0
YCR061W	P25639	0	0.33	YER156C	P40093	0	0
YCR090C	P25654	0	0	YER163C	P32656	0.25	0.31
YCR102C	P25608	0	0	YET1	P35723	0	0.04
YCS4	Q06156	0	0	YET3	Q07451	0	0
YDJ1	P25491	0	0	YFH1	Q07540	0	0
YDL027C	Q07349	0	0	YFH7	P43591	0	0
YDL073W	Q07454	0	0.31	YFL042C	P43560	0	0
YDL086W	Q07505	0	0	YFL067W	P43537	0	0
YDL114W	Q07530	0	0	YGL036W	P53185	0.23	0
YDL121C	Q07541	0	0	YGL039W	P53183	0	0.12
YDL124W	Q07551	0	0.11	YGL041W-A	P0C5N3	0	0
YDL163W	Q12148	0	0	YGL101W	P53144	0	0
YDL233W	Q07684	0	0	YGL140C	P53120	0	0
YDR056C	Q12025	0	0	YGL242C	P53066	0	0
YDR109C	Q04585	0	0	YGL262W	P53054	0	0
YDR161W	Q03771	0	0	YGR001C	P53200	0	0
YDR170W-A	Q03964	0	0.33	YGR012W	P53206	0.23	0
YDR210C-D	Q99231	0.25	0	YGR017W	P53210	0	0
YDR248C	Q03786	0.42	0	YGR021W	P53212	0	0
YDR261C-C	O74302	0.25	0.67	YGR022C	P53213	0	0
YDR261C-D	Q07793	0.25	0	YGR027W-B	Q12141	0	0.33

YGR035W-A	Q45U48	0	0	YJR011C	P47086	0	0
YGR054W	P53235	0	0	YJR030C	P47101	0	0
YGR093W	P53255	0	0	YJR054W	P47114	0	0
YGR111W	P53265	0	0	YJR085C	P47131	0	0.31
YGR117C	P53270	0	0	YJR111C	P47148	0	0
YGR126W	P53274	0	0.31	YJR154W	P47181	0	0
YGR127W	P53275	0	0	YJU3	P28321	0	0
YGR130C	P53278	0	0	YKE2	P52553	0	0
YGR149W	P48236	0	0	YKL027W	P36101	0	0
YGR237C	P50089	0	0	YKL033W-A	Q86ZR7	0	0
YGR250C	P53316	0	0	YKL047W	P36090	0	0
YGR266W	P53326	0	0	YKL050C	P35736	0	0
YGR273C	P53329	0	0	YKL077W	P36081	0	0
YHB1	P39676	0.35	0.33	YKL097C	P34245	0	0
YHL009W-B	P47024	0	0	YKL105C	P34250	0	0
YHM2	Q04013	0	0.33	YKL107W	P34251	0	0
YHP1	Q04116	0	0.31	YKL145W-A	P0C5P3	0	0
YHR003C	P38756	0.18	0	YKL151C	P36059	0	0
YHR020W	P38708	0	0	YKR018C	P36114	0	0
YHR033W	P38690	0.23	0	YKR041W	P36134	0	0
YHR045W	P38775	0.23	0.48	YKR096W	P36168	0	0
YHR080C	P38800	0	0	YKT6	P36015	0	0.01
YHR086W-A	Q3E746	0	0	YLF2	P38746	0	0
YHR131C	P38835	0	0	YLL007C	Q07799	0	0.33
YHR182W	P38870	0	0.31	YLL032C	Q07834	0	0
YIF1	P53845	0.25	0.31	YLR063W	Q12291	0	0
YIL002W-A	Q3E7Z5	0	0.42	YLR143W	Q12429	0	0
YIL082W-A	Q7LHG5	0	0	YLR152C	P54072	0	0
YIL096C	P40493	0	0	YLR173W	Q06247	0	0
YIL108W	P40483	0.01	0.19	YLR177W	Q06251	0	0
YIL151C	P40456	0	0	YLR179C	Q06252	0	0
YIL156W-B	Q2V2P4	0	0	YLR194C	Q05777	0	0
YIL166C	P40445	0	0	YLR202C	O13531	0	0
YIM1	P28625	0	0	YLR241W	Q06538	0	0
YIP1	P53039	0.23	0.31	YLR243W	Q06543	0	0
YIP3	P53633	0	0.08	YLR256W-A	P0C2I8	0.75	0
YIP4	P53093	0	0.34	YLR257W	Q06146	0	0
YIP5	P53108	0	0.23	YLR271W	Q06152	0	0
YIR035C	P40579	0	0	YLR287C	Q05881	0.23	0
YJL070C	P40361	0	0	YLR290C	Q05892	0	0
YJL107C	P42947	0	0	YLR361C-A	Q3E795	0	0.31
YJL171C	P46992	0	0.02	YLR366W	Q7LIF1	0.4	0
YJL185C	P46983	0	0	YLR413W	Q06689	0.17	0.23

YLR415C	O13578	0	0	YNL284C-A	Q12391	0.25	0.33
YLR419W	Q06698	0	0	YNL284C-B	Q12112	0	0
YLR460C	P54007	0	0	YNL295W	P48564	0	0
YME1	P32795	0	0.16	YNR021W	P53723	0.15	0.2
YME2	P32843	0	0	YNR029C	P53729	0	0.33
YML002W	P0CF17	0	0	YNR034W-A	Q3E841	0	0.31
YML039W	Q03434	0	0	YNR061C	P53747	0	0
YML099W-A	Q6B2I9	0	0	YNR063W	P53749	0	0
YML119W	Q03208	0	0	YOL073C	Q08232	0	0
YML6	P51998	0	0	YOL075C	Q08234	0	0
YMR010W	Q03687	0	0	YOL098C	Q12496	0	0
YMR018W	Q04364	0	0	YOL103W-A	Q92392	0	0.33
YMR027W	Q04371	0	0	YOL103W-B	Q12273	0	0.33
YMR045C	Q04214	0	0	YOL150C	Q08293	0	0
YMR046C	Q04215	0	0.33	YOL155W-A	Q3E7Y8	0	0
YMR074C	Q04773	0	0	YOP1	Q12402	0	0
YMR086W	Q04279	0	0	YOR019W	Q99248	0	0
YMR087W	Q04299	0	0	YOR021C	Q12314	0.01	0
YMR099C	Q03161	0.22	0.03	YOR062C	P36025	0	0
YMR102C	Q03177	0	0	YOR093C	Q12275	0	0.55
YMR130W	Q04223	0	0	YOR1	P53049	0	0
YMR178W	Q03219	0.33	0	YOR111W	Q99210	0	0
YMR185W	Q12751	0	0	YOR169C	Q08540	0	0
YMR196W	Q04336	0	0	YOR186C-A	Q8TGL3	0	0
YMR221C	Q04991	0.48	0.33	YOR223W	Q12015	0	0
YMR226C	Q05016	0	0	YOR296W	Q08748	0	0
YMR245W	Q04019	0	0	YOR352W	Q08816	0	0
YMR259C	Q03496	0.25	0	YOS1	Q3E834	0	0
YMR315W	Q04869	0.5	0.66	YOS9	Q99220	0	0
YMR317W	Q04893	0.25	0	YPK1	P12688	0.37	0.49
YNK1	P36010	0	0	YPK3	P38070	0.25	0
YNL010W	P53981	0.25	0	YPK9	Q12697	0	0
YNL011C	P53980	0	0	YPL088W	Q02895	0	0
YNL035C	P53962	0.42	0.31	YPL199C	Q08954	0	0
YNL040W	P53960	0	0	YPL225W	Q08971	0	0
YNL092W	P53934	0	0	YPL257W-B	Q12414	0	0
YNL144C	P53907	0	0	YPL260W	Q08977	0	0
YNL155W	P53899	0	0	YPP1	P46951	0	0
YNL193W	P53870	0	0	YPR010C-A	A5Z2X5	0	0
YNL198C	P40166	0	0	YPR022C	Q12139	0.23	0
YNL208W	P40159	0	0	YPR059C	P0C5E1	0.23	0
YNL234W	P53857	0	0	YPR063C	Q12160	0	0.33
YNL247W	P53852	0.03	0	YPR077C	O13583	0	0

YPR078C	Q06813	0	0	YRO2	P38079	0	0.33
YPR091C	Q06833	0	0.28	YSC84	P32793	0	0.29
YPR097W	Q06839	0	0	YSP2	Q06681	0	0
YPR1	Q12458	0	0	YSR3	P23501	0.23	0
YPR109W	Q06104	0	0	YTA12	P40341	0	0
YPR117W	Q06116	0	0	YTA7	P40340	0	0.55
YPR137C-B	P0C2I9	0.5	0.33	YTM1	Q12024	0	0
YPR137C-B	Q99337	0	0	YVH1	Q02256	0	0
YPR147C	Q06522	0	0.33	ZDS1	P50111	0	0
YPR148C	Q06523	0	0	ZDS2	P54786	0	0
YPS7	Q06325	0	0	ZEO1	Q08245	0	0
YPT1	P01123	0	0	ZIM17	P42844	0	0
YPT10	P38146	0	0	ZIP2	P53061	0	0
YPT31	P38555	0	0	ZPR1	P53303	0	0
YPT32	P51996	0	0	ZRC1	P20107	0	0
YPT52	P36018	0	0	ZTA1	P38230	0	0
YPT7	P32939	0	0	ZUO1	P32527	0	0.27
YRA1	Q12159	0	0.01	ZWF1	P11412	0.48	0
YRA2	P36036	0	0				
YRB1	P41920	0	0				
YRB2	P40517	0	0				
YRB30	P53107	0	0				
YRM1	Q12340	0	0				

REFERENCES

Ando, A. Nakamura, T. Murata, Y. Takagi, H. Shima, J. (2007). Identification and Classification of Genes Required for Tolerance to Freeze-Thaw Stress Revealed by Genome-Wide Screening of *Saccharomyces cerevisiae* Deletion Strains. *FEMS Yeast Research.* 7:2. 244-53.

Amerik, AY. Li, SJ. Hochstrasser, M. (2000). Analysis of the Deubiquitinating Enzymes of the Yeast *Saccharomyces cerevisiae*. *Biological Chemistry*. 381:9-10. 981-92.

Athenstaedt, K. Daum, G. (2005). Tgl4p and Tgl5p, Two Triacylglycerol Lipases of the Yeast Saccharomyces cerevisiaeare localize to lipid particles. Journal of Biological Chemistry. 280:45. 37301-9.

Awrey, DE. Weilbaecher, RG. Hemming, SA. Orlicky, SM. Kane, CM. Edwards, AM. (1997). Transcription Elongation Through DNA Arrest Sites: A Multistep Process Involving Both RNA Polymerase II Subunit Rpb9 and TFIIS. *Journal of Biological Chemistry.* 272:23. 14747-14754.

Bayev, AA. Georgiev, OI. Hadjiolov, AA. Kermekchiev, MB. Nikolaev, N. Skryabin, KG. Zakharyev, VM. (1980). The Structure of the Yeast Ribosomal RNA Genes. 2. The Nucleotide Sequence of the Initiation Site for Ribosomal RNA Transcription. *Nucleic Acids Research.* 8:21. 4979-26.

Belden, WJ. Barlowe, C. (1996). Erv25p, a component of COPII-Coated Vesicles, Forms a Complex with Emp24p That is Required for Efficient Endoplasmic Reticulum to Golgi Transport. Journal of Biological Chemistry. 251:43. 26939-46.

Brenner, S. Jacob, F. Meselson, M. (1961). An Unstable Intermediate Carrying Information from Genes to Ribosomes for Protein Synthesis. *Nature.* 13. 576-581.

Bram, RJ. Kornber, RD. (1985). Specific Protein Binding to Far Upstream Activating Sequences in Polymerase II Promoters. *Proceedings of the National Academy of Sciences of the United States of America.* 82:1. 43-7.

Cedar, H. Solage, A. Zurucki, F. (1976). Control of the RNA Synthesis by Chromatin Proteins. *Nucleic Acid Research.* 3:7. 1659-70.

Chymkowitch, P. Eldholm, V. Lorenz, S. Zimmermann, C. Lindvall, JM. Bjoras, M. Meza-Zepeda, LA. Enserink, JM. (2012). Cdc28 Kinase Activity Regulates the Basal Transcription Machinery at a Subset of Genes. *Proceedings of the National Academy of Sciences of the United States of America.* 109:26. 10450-5.

Cohen, A. Perzov, N. Nelson, H. Nelson, N. (1999). A Novel Family of Yeast Chaperons Involved in the Distribution of V-ATPase and Other Membrane Proteins. *Journal of Biological Chemistry.* 274:38. 26885-93.

Cosma, MP. Panizza, S. Nasmyth, K. (2001). Cdk1 Triggers Association of RNA Polymerase t Cell Cycle Promoters Only After Recruitment of the Mediator by SBF. *Molecular Cell.* 7:6. 1213-20.

Copic, A. Dorrington, M. Pagant, S. Barry, J. Lee, MC. Singh, I. Hartman, JL 4th. Miller, EA. (2009). Genomwide Analysis Reveals Novel Pathways Affecting Endoplasmic Reticulum Homeostasis, Protein Modification, and Quality Control. Genetics. 182:3. 757-69.

Crick, FH. (1968). The Origin of the Genetic Code. *Journal of Molecular Biology.* 38:3. 367-79.

De Winde, JH. Cruwels, M. Hohmann, S. Thevelein, JM. Winderickx, J. (1996). Differential Requirement of the Yeast Suga Kinases for Sugar Sensing in Establishing the Catabolite-Repressed State. *European Journal of Biochemistry*. 241:2. 633-43.

Deshaies, RJ. Schekman, R. (1987). A Yeast Mutant Defective at an Early Stage in Import of Secretory Protein Precursors into the Endoplasmic Reticulum. Journal of Cell Biology. 105:2. 622-45.

Desmoucelles, C. Pinson, B. Saint-Mare, C. Daignan-Fornier, B. Screening the Yeast "DIsruptome" for Mutants Affecting Resistance to the Immunosuppressive Drug, Mycophenolic Acid. *Journal of Biological Chemistry.* 277:30. 27036-27044.

Ding, B. Ruggiero, C. Chen, X. Li, S. (2007). Tfb5 is Partially Dispensable for Rad26 Mediated Transcription Coupled Nucleotide Excision Repair in Yeast. *DNA Repair*. 6:11. 1661-9.

Duttler, S. Pechmann, S. Frydman, J. (2013). Principles of Cotranslational Ubiquitination and Quality Control at the Ribosome. *Molecular Cell.* 50:3. 379-93.

Exinger, F. Lacroute, F. (1992). 6-Azauracil Inhibition of GTP Biosynthesis in *Saccharomyces cerevisiae.* Current Genetics. 22:1. 9-11.

Garcia-Ramirez, JJ. Santos, MA. Revuelta, JL. (1995). The Saccharomyces cerevisiae RIB4 Gene Codes for 6,7-Dimethyl-8-ribityllumazine Synthase Involved in Riboflavin Biosynthesis. Journal of Biological Chemistry. 270,40. 23801-7.

Gardiner, FC. Costa, R. Ayschough, KR. (2007). Nucleotytoplasmic Trafficking is Required for Functioning of the Adaptor Protein Sla1p in Endocytosis. *Traffic*. 8:4. 347-58.

Gavin, AC. Aloy, P. Grandi, P. Krouse, R. Boesche, M. Marzioch, M. Rau, C. Jensen, LJ. Bastuck, S. Dumplefeld, B. Edelmann, A. Hertier, MA. Hoffman, V. Hoefert, C. Klein, K. Hudak, M. Michon, AM. Schelder, M. Schirle, M. Remor, M. Rudi, T. Hooper, S. Bauer, A. Bouwmeester, T. Casari, G. Drewes, G. Neubauer, G. Rick, JM. Kuster, B. Bork, P. Russell, RB Superti-Furga, G. (2006). Proteome Survey Reveals Modularity of the Yeast Cell Machinery. *Nature*. 440:7084. 631-6.

Gavin, AC. Maeda, K. Kuhner, S. (2011). Recent Advances in Charting Protein-Protein Interactions: Mass Spectrometry-Based Approaches. *Current Opinions in Biotechnology.* 22:1. 42-9.

Gemmill, TR. Wu, X. Hanes, SD. (2005). Vanishingly Low Levels of Ess1 Prolyl-Isomerase Activity are Sufficient for Growth in Saccharomyces Cerevisiae. *Journal of Biological Chemistry.* 280:16. 15510-7.

Gibney, PA. Fries, T. Bailer, SM. Morano, KA. (2008). Rtr1 is the *Saccharomyces cerevisiae* Homolog of a Novel Family of RNA Polymerase II-Binding Proteins. *Eukaryotic Cell*. 7:6. 938-48.

Gilmore, JM. Sardiu, ME. Venkatsh, S. Stutzman, B. Peak, A. Seidel, CW. Workman, JL. Florens, L. Washburn, MP. (2012). Characterization of a Highly Conserved Histone Related Protein, Ydl156w, and Its Functional Associations Using Quantitative Proteomic Analyses. *Molecular and Cellular Proteomics.* 11:4.

Hahn, S. Young, ET. (2011). Transcriptional Regulation in *Saccharomyces cerevisiae*: Transcription Factor Regulation and Function, Mechanisms of Initiation, and Roles of Activators and Coactivators. *Genetics*. 189:3. 705-36.

Hanawalt, PC. (2001). Controlling the Efficiency of Excision Repair. *Mutation Research.* 485:1. 3-13.

Hemming, SA. Jansma, DB. Macgregor, PF. Goryachev, A. Friesen, JD. Edwards, AM. (2000). RNA Polymerase II Subunit Rpb9 Regulates Transcription Elongation *in Vivo*. *Journal of Biochemistry.* 275:45. 35506-35511.

Ho, Y. Gruhler, A. Heilbut, A. Bader, GD. Moore, L. Adams, SL. Millar, A. Taylor, P. Bennett, K. Boutilier, K. Yang, L. Wolting, C. Donaldson, I. (2002). Systematic Identification of Protein Complexes in *Saccharomyces cerevisiae* by Mass Spectrometry. *Nature*. 415:6868. 180-3.

Holtzman, DA. Yang, S. Drubin, DG. (1993). Syntheic-Lethal Interactions Identify Two Novel Genes, SLA1 and SLA2, that Control Membrane Cytoskeleton Assembly in Saccharomyces Cerevisiae. *Journal of Cell Biology.* 122:3. 635-44.

Howard, JP. Hutton, J. Olson, JM. Payne, GS. (2002). Sla1p Serves as the Targeting Signal Recognition Factor for NPFX(1,2)D-Mediated Endocytosis. *Journal of Cell Biology*. 157:2. 315-26.

Kaksonen, M. Toret, CP. Drubin, DG. (2005). A Modular Design for the Clarthrin- and Actin-Mediated Endocytosis Machinery. *Cell*. 123:2. 305-20.

Kalies, KU. Allan, S. Sergeyenko, T. Kröger, H. Römisch, K. (2005). The Protein Translocation Channel Binds Proteasomes to the Endoplasmic Reticulum Membrane. The EMBO Journal. 24:13. 2284-93.

Kainov, DE. Seth, LA. Svejstrup, JQ. Egly, JM. Poterzsman, A. (2009). Interacting Partners of the Tfb2 Subunit from Yeast TFIIH. *DNA Repair.* 9:1. 33-9.

Komarnitsky, P. Cho, EJ. Buratowski, S. (2000). Different Phosphorylated Forms of RNA Polymerase II and Associated mRNA Processing Factors During Transcription. Genes and Development. 14. 2452-60.

Knippa, K. Peterson, DO. (2013). Fidelity of RNA Polymerase II Transcription: Role of Rbp9 in Error Detection and Proofreading. *Biochemistry.* 52. 7807-17.

Krogan, NJ. Cagney, G. Yu, H. Zhong, G. Guo, X. Ignatchenko, A> Li, J. Pu, S. Datta, N. Tiuisis, AP. Punna, T. Peretrin-Alvarez, JM. Shales, M. Zhang, X. Davey, M. (2006). Global Landscape of Protein Complexes in the Yeast *Saccharomyces cerevisiae*. *Nature*. 440:7084. 637-43.

Kurat, CF. Wolinski, H. Petschnigg, J. Kaluarachchi, S. Andrews, B. Natter, K. Kohlwein, SD. (2009). Cdk1/Cdc28-Dependent Activation of the Major Triacylglycerol Lipase Tgl4 in Yeast Links Lipolysis to Cell-Cycle Progression. *Molecular Cell*. 33:1. 53-63.

Kvint, K. Uhler, JP. Taschner, MJ. Sigurdsson, S. Erdjument-Bromage, H. Tempst, P. Svejstrup, JQ. (2008). Reversal of RNA Polymerase II Ubiquitylation by the Ubiquitin Protease Ubp3. *Molecular Cell*. 30:4. 498-506.

Li, S. Smerdon, MJ. (2002). Rpb4 and Rpb9 Mediate Subpathways of Transcription-Coupled DNA Repair in *Saccharomyces cerevisiae. EMBO Journal.* 21:21. 5921-5929.

Lobo, Z. Maitra, PK. (1977). Physiological Role of Glucose-Phosphorylating Enzymes in *Saccharomyces Cerevisiae*. *Archives of Biochemistry and Biophysics.* 182:2. 639-45.

Ma, Z. Atencio, D. Barnes, C. DeFiglio, H. Hanes, SD. (2012). Multiple Roles for the Ess1 Prolyl Isomerase in the RNA Polymerase II Transcription Cycle. *Molecular and Cellular Biologh*. 32:17. 3594-607.

Mayor, T. Graumann, J. Bryan, J. MacCoss, MJ. Deshaies, RJ. (2007). Quantitative Profiling of Ubiquitylated Proteins Reveals Proteasome Substrates and the Substrate Repertoire Influenced by the Rpb10 Receptor Pathway. *Molecular & Cellular Proteomics.* 6:11. 1885-95.

Marzioch, M. Henthorn, DC. Herrmann, JM. Wilson, R. Thomas, DY. Bergeron, JJ. Solari, RC. Rowley, A. (1999). Erp1p and Erp2p, partners for Emp24p and Erv25p in a yeast p24 complex. Molecular Biology of the Cell. 10:6. 1923-38.

McKune, K. Moore, PA. Hull, MW. Woychik, NA. (1995). Six Human Polymerase Subunits Functionally Substitute for Their Yeast Counterparts. *Molecular and Cellular Biology.* 15:12. 6895-900.

Mellacheruvu, D. Wright, Z. Couzens, A. Lambert, J. St-Denis, N. Li, T. Miteva, Y. Hauri, S. Sardiuj, M. Low, T. Halim, V. Bagshaw, R. Hubner, N. Hakim, A. Bouchard, A. Faubert, D. Fermin, D. Dunham, W. Goudreault, M. Lin, Z. Badillo, B. Pawson, T. Durocher, D. Coulombe, B. Aebersold, R. Furga, G. Colinge, J. Heck, A. Choi, H. Gstaiger, M. Mohammed, S. Cristea, I. Bennett, K. Washburn, M. Raught, B. Ewing, R. Gingras, AC. Nesvizhskii, A. (2013). The CRAPome: a Contaminant Repository for Affinity Purification Mass Spectrometry Data. Nature Methods 10:9 730–6.

Mitchell, SF. Jain, S. She, M. Parker, R. (2013). Global Analysis of Yeast mRNPs. *Nature Structural and Molecular Biology*. 20:1. 127-33.

Mochida, J. Yamamoto, T. Fujimura-Kamada, K. Tanaka, K. (2002). The Novel Adaptor Protein, Mti1p, and Rrp1p, a homolog of Wiskott-Aldrich Syndrome Protein-Interaction Protein (WIP), May Antagonistically Regulate Type 1 Myosin in *Saccharomyces cerevisiae*. *Genetics*. 160:3. 923-34.

Mosley, AL. Pattenden, SG. Carey, M. Venkatesh, S. Gilmore, JM. Florens, L. Workman, JL. Washburn, MP. (2009). Rtr1 is a CTD Phosphatase That Regulates RNA Polymerase II During the Transition from Serine 5 to Serine 2 Phosphorylation. Molecular Cell. 34. 168-178.

Mosley, AL. Sardiu, ME. Pattenden, SG. Workman, JL. FLorens, L. Washburn, MP. (2011). Highly Reproducible Label Free Quantitative Proteomic Analysis of RNA Polymerase Complexes. *Molecular & Cellular Proteomics.* 10:2.

Morris, CP. Lim, F. Wallace, JC. (1987). Yeast Pyruvate Carboxylase: Gene Isolation. *Biochemical and Biophysical Research Communications.* 145:1. 390-6.

Müller, O. Bayer, MJ. Peters, C. Andersen, JS. Mann, M. Mayer, A. (2002). The Vtc Proteins in Vacuole Fusion: Coupling NSF Activity to V(0) Trans-Complex Formation. *EMBO Journal.* 21:3. 259-69.

Nakahara, K. Ohkuni, A. Kitamura, T. Abe, K. Naganuma, T. Ohno, Y. Zoeller, RA. Hihara, A. (2012). The Sjögren-Larsson Syndrome Gene Encodes a Hexadecenal Dehydrogenase of the Sphingosine 1-Phosphate Degradation Pathway. *Molecular Cell.* 46. 461-71.

Nesser, NK. Peterson, DO. Hawley, DK. (2006) RNA Polymerase II Subunit Rpb9 is Important for Transcriptional Fidelity In Vivo. Proceedings of the National Academy of Science. 103:9. 3268-3272.

Ostapenko, D. Burton, JL. Solomon, MJ. (2015). The Ubp15 Deubiquitinase Promotes Timely Entry into S Phase in *Saccharomyces cerevisiae*. *Molecular Biology of the Cell.* 26:12. 2205-16.

Ossareh-Nazari, B. Bonizec, M. Cohen, M. Dokudovskaya, S. Delande, F. Schaeffer, C. Van Dorsselear, A. Dargemenot, C. (2010). Cdc48 and Ufd3, New Partners of the Ubiquitin Protease Ubp3, are Required for Ribophagy. *EMBO Reports*. 11:7. 548-54.

Peng, J. Schwartz, D. Elias, JE. Thoreen, CC. Cheng, D. Marsischky, G. Roelofs, J. Finley, D. Gygi, SP. (2003). A Proteomics approach to Understanding Protein Ubiquitination. *Nature Biotechnology.* 21:8. 921-6.

Phatnani, HP. Jones, JC. Greenleaf, AL. (2004). Expanding the Functional Repertoire of CTD Kinase I and RNA Polymerase II: Novel PhosphoCTD-associating Proteins in the Yeast Proteome. *Biochemistry.* 43:50. 15702-19.

Porrua, O. Libri, D. (2013). A Bacterial-Like Mechanism for Transcription Termination by the Sen1p Helicase in Budding Yeast. Nature Structural & Molecular Biology. 20. 884-91.

Prinz, A. Hartmann, E. Kalies, KU. (2000). Sec61p is the Main Ribosome Receptor in the Endoplasmic Reticulum of Saccharomyces cerevisiae. Biological Chemistry. 381:9-10. 1025-9.

Rajakumari, S. Daum, G. (2010). Multiple Functions as Lipase, Steryl Ester Hydrolase, Phospholipase, and Acyltransferase of Tgl4p from the Yeast *Saccharomyces cerevisiae*. *Journal of Biological Chemistry.* 285:21. 5769-76.

Rodriguez, A. De la Cera, T. Herrero, P. Moreno, F. (2001). The Hexokinase 2 Protein Regulates the Expression of the GLK1, HXK1, and HXK2 genes of *Saccharomyces cerevisiae*. *The Biochemical Journal*. 355:3. 625-21

Sainsbury, S. Niesser, J. Cramer, P. (2013). Structure and Function of the Initially Transcribing RNA Polymerase II-TFIIB Complex. *Nature.* 493:7432. 437-40.

Schlecht, U. Miranda, M. Suresh, S. Davis, RW. St. Onge, RP. (2012). Multiplex Assay for Condition-Dependent Changes in Protein-Protein Interactions. *Proceedings of the National Academy of Sciences of the United States of America.* 109:23. 9213-8.

Schlösser, T. Wiesenburg, A. Gätgens, C. Dunke, A. Viets, U. Vijayalakshmi, S. Nieland, S.

Stahmann, KP. (2007). Growth Stress Triggers Riboflavin Overproduction in *Ashbya gossypii. Applied Microbiological Biotechnology.* 76. 569-78.

Shen, Z. St-Denis, A. Chartrand, P. (2010). Cotranscriptional Recruitment of She2p by RNA Pol II Elongation Factor Spt4-Spt5/DSIF Promotes mRNA Localization to the Yeast Bud. *Genes and Development*. 24:17. 1914-26.

Steinmetz, EJ. Warren, CL. Kuehner, JN. Panbehi, B. Ansari, AZ. Brow, DA. (2006). Genome-Wide Distribution of Yeast RNA Polymerase II and Its Control by Sen1 Helicase. Molecular Cell. 24:5. 735-46.

Stucka, R. Dequin, S. Salmon, JM> Gancedo, C. (1991). DNA Sequence in Chromosomes II and VII Code for Pyruvate Carboxylase Isoenzymes in Saccharomyces Cerevisiae: Analysis of Pyruvate Carboxylase-Deficient Strains. *Molecular and General Genetics.* 229:2. 307-15.

Tarassov, K. Messier, V. Landry, CR. Radinovic, S. Serna Molina MM. Shames, I. Malitskaya, Y. Vogel, J. Bussey, H. Michnick, SW. (2008). An *In Vivo* Map of the Yeast Protein Interactome. *Science.* 320:5882. 1465-70.

Tkach, JM. Yimit, A. Lee, AY. Riffle, M. Costanzo, M. Jaschob, D. Hendry, JA. Ou, J. Moffat, J. Boone, C. Davis, TN. Nislow, C. Brown, GW. (2012). Dissecting DNA Damage Response Pathways by ANalysing Protein Localization and Abundance Changes During DNA Replication Stress. *Nature Cell Biology.* 14:9. 966-76.

Tong, AH. Drees, B. Nardelli, G. Bader, GD. Brannetti, B. Castagnoli, L. Evangelista, M. Ferracuit, S. Nelson, B. Paoluzi, S. Quondam, M. Zucconi, A. Hogue, CW. Fields, S. Boone, C. Cesareni, G. (2002). A Combined Experimental and Computational Strategy to Define Protein Interaction Networks for Peptide Recognition Modules. *Science*. 295:5553. 321-4.

Ubersax, JA. Woodbury, EL. Quang, PN. Paraz, M. Blethrow, JD. Shah, K. Shokat, KM. Morgan, DO. (2003). Targets of the Cyclin-Dependent Kinase Cdk1. *Nature*. 425:6960. 859-64.

Ursic, D. Chinchila, K. Finkel, JS. Culbertson, MR. (2004). Multiple Protein/Protein and Protein/RNA Interactions Suggest Roles for Yeast DNA/RNA Helicase Sen1p in Transcription, Transcription-coupled DNA Repari, and RNA Processing. *Nucleic Acid Research.* 32:8. 2441-52.

Vasiliou, V. Pappa, A. Petersen, DR. (2000.) Role of Aldehyde Dehydrogenase in Endogenous and Xenobiotic Metabolism. *Chemico-Biological Interactions.* 129. 1-19.

Warren, DT. Andrews, PD. Gourlay, CW. Ayscough, KR. (2002). Sla1p Couples the Yeast Endocytic Machinery to Proteins Regulating Actin Dynamics. *Journal of Cell Science.* 115:8. 1703-15.

West, MG. Barlow, CK. Appling, DR. (1993). Cloning and Characterization of the *Saccharomyces cerevisiae* Gene Encoding NAD-dependent 5,10-Methylenetetrahydrofolate Dehydrogenase. *Journal of Biological Chemistry.* 286:1. 153-160.

West, ML. Corden, JL. (1995). Construction and Analysis of Yeast RNA Polymerase II CTD Deletion and Substitution Mutations. *Genetics*. 140:4. 1223-33.

Wimberly, BT. Brodersen, DE. Clemons, WM Jr. Morgan-Warren, RJ. Carter, AP. Vonrhein, C. Hartsch, T. Ramakrishnan, V. (2000). Structure of the 30 S Ribosomal Subunit. *Nature.* 407:6802. 327-39.

Woychik, NA. Hampsey, M. (2002). The RNA Polymerase II Machinery: Structure Illuminates Function. *Cell.* 108:4. 453-63.

Woychik, NA. Lane, WS. Young, RA. (1991). Yeast RNA Polymerase II Subunit Rpb9 is Essential for Growth at Temperature Extremes. *Journal of Biological Chemistry.* 266:28. 19053-5.

Wu, X. Wilcox, CB. Devasahayam, G. Hackett, RL. Arevalo-Rodriquez, M. Cardenas, ME. Heitman, J. Hanes, SD. (200). The Ess1 Prolyl Isomerase is Linked to Chromatin Remodeling Complexes and the General Transcription Machinery. *The EMBO Journal*. 19:14. 3727-38.

Zahedi, RP. Sickmann, A. Boehm, AM. Winkler, C. Zufall, N. Schonfisch, B. Guiard, B. Pfanner, N. Meisinger, C. (2006). Proteomic Analysis of the Yeast Mitochondrial Outer Membrane Reveals Accumulation of a Subclass of Preproteins. Molecular Biology of the Cell. 17. 1436-1450.

Ziv, I. Matiuhin, Y. Kirkpatrick, DS. Erpapazoglou, Z. Leon, S. Pantazopoulou, M. Kim, W. Gygi, SP. Haquenauer-Tsapis, R. Reis, N. Glickman, MH. Kleifeld, O. (2011). A Perturbed Ubiquitin Landscape Distinguishes Between Ubiquitin in Trafficking and in Proteolysis. *Molecular & Cellular Proteomics.* 10:5.

CURICULUM VITAE
Eric A Talbert

Education

Master of Science in Biochemistry and Molecular Biology
Indiana University, Indianapolis, IN
Thesis: Changes in the Rpb3 Interactome Caused by the Deletion of *rpb9* in *Saccharomyces Cerevisiae*

Bachelor of Science in Microbiology
Purdue University, West Lafayette, IN

Bachelor of Science in Biochemistry
Purdue University, West Lafayette, IN
Minor in Chemistry

Professional History

Volunteer Coordinator
Wildfire, LLC
December, 2015-Current

- Assist Head of Organized Play in scheduling gameplay events for conventions
- Act as liaison between convention volunteers and core management
- Run gameplay events to showcase products during conventions
- Take part in and assist in directing discussion during weekly online product testing meetings

Starts Technician/Quality Assurance and Food Testing Technician
Vivolac Cultures Corporation
October 2012-September 2013

- Prepared inoculum daily for production tanks from frozen and freeze dried seed
- Maintained the Vivolac library of frozen seed cultures
- Tested both internally produced and independently submitted samples for contamination

Chromatography Chemist
Cogent, LLC
October 2011- May 2012

- Performed flash chromatography and HPLC purification in support of medicinal chemists developing novel molecules
- Determined identity of purified samples using LC/MS analysis.

Undergraduate Intern
NOX Technologies, Inc.
January 2011-May2011

- Performed spectrophotometry to assay activity of protein arNOX

Undergraduate Research Assistant
Purdue University Department of Medicinal Chemistry and Molecular Pharmacology
August 2007-June 2009
Under Dr. D. James Morré, West Lafayette, Indiana.
Summer 2008 paid for by Howard Hughes Undergraduate Internship.

- Prepared HeLa cell microsome supernatant using centrifugation
- Performed gel electrophoresis, Western blotting and HPLC

Other Awards
Howard Hughes Undergraduate Internship (2008)
Eagle Scout (2005)